



Review of the state of current knowledge regarding tyre braking performance, anti-skid systems, and modern aircraft tyres on water contaminated runways

G.W.H. van Es

Short abstract: Future Sky Safety is a Joint Research Programme (JRP) on Safety, initiated by EREA, the association of European Research Establishments in Aeronautics. The Programme contains two streams of activities: 1) coordination of the safety research programmes of the EREA institutes and 2) collaborative research projects on European safety priorities.

This deliverable is produced by Future Sky Safety Project P3 Solutions for Runway Excursions. This study gives the current knowledge on tyre braking performance, anti-skid systems, and modern aircraft tyres on water contaminated runways.

Programme Manager	M.A. Piers, NLR
Operations Manager	L.J.P. Speijker, NLR
Project Manager (P3)	G.W.H. van Es, NLR
Grant Agreement No.	640597
Document Identification	D3.3
Status	Approved
Version	2.0
Classification	Public

This page is intentionally left blank

Contributing partners

Company	Name
NLR	Gerard van Es
Airbus SAS	Matthieu Mayolle
Airbus Defence & Space	Felix Delgado
INCAS	Stefan Bogos

Document Change Log

Version	Issue Date	Remarks
1.0	04-12-2015	First formal release
1.1	10-12-2015	Update by Operations Manager (NLR)
2.0	17-12-2015	Second formal release

Approval status

Prepared by: (name)	Company	Role	Date
G.W.H van Es	NLR	Main Author	04-12-2015
Checked by: (name)	Company	Role	Date
H. Smit	NLR	Quality Assurance	04-12-2015
Approved by: (name)	Company	Role	Date
G.W.H. van Es	NLR	Project Manager (P3)	04-12-2015
L.J.P. Speijker	NLR	Operations Manager	22-12-2015

Acronyms

Acronym	Definition
EASA	European Aviation Safety Agency
ESDU	Engineering Sciences Data Unit
FAA	Federal Aviation Administration
NASA	National Aeronautics and Space Administration
NLR	National Aerospace Laboratory

EXECUTIVE SUMMARY

Problem Area

The vast majority of aircraft takeoffs and landings are conducted on dry runways. Only a small portion is conducted on non-dry runways like water contaminated (flooded) runways. Statistics show that the likelihood of a runway excursion during takeoff or landing is much higher on flooded runways than on dry runways. Extreme loss of tyre braking can occur during rejected takeoffs and landings on flooded runways. As a result the stopping distance increases significantly which could exceed the available runway length. Most research in the past has focused on the braking capabilities of aircraft on wet runways instead of water contaminated runways. Most of the knowledge of aircraft braking performance on water contaminated runways was gained during the late 60s and mid-70s. This knowledge is still used to determine the takeoff and landing performance of today's modern aircraft. During the development of the European Action Plan for the Prevention of Runway Excursions it was recognised that current aircraft designs may act differently when braking on water contaminated runways, from aircraft tested in the 60s and 70s.

Description of Work

A literature study is conducted, with the aim to describe the state of current knowledge regarding tyre braking performance, anti-skid systems, and modern aircraft tyres on water contaminated runways. Information and data mainly coming from public sources are used to describe the state of current knowledge. Also data from older studies are considered as such data are often still the basis of the current knowledge and means of compliance used in aircraft performance analysis and certification.

Results & Conclusions

This report summarises the state of current knowledge regarding tyre braking performance, anti-skid systems, and modern aircraft tyres on water contaminated runways.

The factors that influence aircraft tyre braking performance on water contaminated runways are discussed in detail. Influence of tyre design and runway texture is explained.

Different anti-skid systems are presented and their performance on slippery surfaces like water contaminated runways is discussed. This shows that modern anti-skid systems are as efficient on slippery runways (like water contaminated runways) as on dry runways, in contrast to the older anti-skid designs.

Finally experimental data of aircraft tyres braked on water contaminated runways are collected. Both data from full-scale tests as well as data from dynamic load tracks are considered. A database is created with information on recorded braking friction values of a large number of aircraft tyres on

water contaminated runways for a range of conditions. This database can be used in later analysis on aircraft stopping performance. The analysed data revealed that there is little information on braking friction on water contaminated runways of aircraft with modern anti-skid systems. Full scale flight tests with two aircraft, as planned in Future Sky Safety Project P3, will help to extend the data in this area.

Applicability

The results of the literature study presented in this report and the friction data of aircraft tyres on water contaminated runways can be used to review and improve current EASA means of compliance related to contaminated runway performance. This activity is planned as follow-up step in the FSS Project P3.

This page is intentionally left blank

TABLE OF CONTENTS

Contributing partners	3
Document Change Log	3
Approval status	3
Acronyms	4
Executive Summary	
Problem Area	5
Description of Work	5
Results & Conclusions	5
Applicability	6
List of Figures	10
List of Tables	12
1 Introduction	13
1.1. The Programme	13
1.2. Project context	13
1.3. Research objectives	14
1.4. Approach	14
1.5. Structure of the document	15
2 braking traction of aircraft tyres on water contaminated runways	16
2.1. General introduction	16
2.2. The 3-zone concept	17
2.3. Influence of runway macro- and microtexture on braking friction	23
3 Anti-skid systems	26
3.1. Introduction	26
3.2. Description of different anti-skid systems and their performance on slippery runways	29
3.3. Modern anti-skid design characteristics	36
4 Dynamic hydroplaning of modern aircraft tyres	39
5 Review of experimental data on braking capabilities of aircraft tyres on flooded runways	46
5.1. Data sources	46
5.2. Short analysis of available data	49

5.2.1. Full-scale aircraft tests	49
5.2.2. Single tyre tests	52
5.3. Remarks on the available braking friction data on water contaminated runways	56
6 Conclusions	58
7 References	59

LIST OF FIGURES

FIGURE 1: EXAMPLE OF AIRCRAFT TYRES BRAKING ON A VERY WET RUNWAY.	17
FIGURE 2: ZONES UNDER A TYRE FOOTPRINT WHEN ROLLING ALONG A WET/FLOODED SURFACE.	18
FIGURE 3: TYRE TREADS OF AIRCRAFT AND CAR TYRES.	21
FIGURE 4: ILLUSTRATION OF MACRO- AND MICROTEXTURE ON A RUNWAY SURFACE [VAN ES AND GIESBERTS, (2003)].....	22
FIGURE 5: INFLUENCE OF RUNWAY TEXTURE ON TYRE-GROUND BRAKING FRICTION AS FUNCTION OF GROUND SPEED.	23
FIGURE 6: COMPARISON OF THE MAXIMUM BRAKING FRICTION COEFFICIENT AS FUNCTION OF GROUND SPEED OF A SINGLE TYRE ON A DRY, WET, AND FLOODED SURFACE [TANNER ET. AL. (1981)].	24
FIGURE 7: COMPARISON OF THE EFFECTIVE BRAKING FRICTION COEFFICIENT AS FUNCTION OF GROUND SPEED ON A DRY, WET, AND FLOODED RUNWAY FOR A B737-100 [YAGER ET. AL. (1990)].....	25
FIGURE 8: RELATION BRAKING FRICTION AND SLIP RATIO [SEE E.G. HOLMES (1970)].	26
FIGURE 9: ILLUSTRATION OF INFLUENCE OF RUNWAY CONDITION ON MU SLIP RATIO RELATION.	27
FIGURE 10: ILLUSTRATION OF THE FUNCTIONING OF AN ANTI-SKID SYSTEM [ELLIOT AND DeVLIEG (1978)].	28
FIGURE 11: EXAMPLE OF AN ANTI-SKID WORKING ON A FLOODED RUNWAY (SOURCE: COLOMBIA, AERONAUTICA CIVIL, ACCIDENT REPORT, ERJ-145 HK 4536, 2010).	29
FIGURE 12: EXAMPLE OF WHEEL BRAKE FORCE AND WHEEL SPEED TIME TRACES FOR AN ON-OFF ANTI-SKID SYSTEM [MITCHELL, (1995)].....	30
FIGURE 13: EXAMPLE OF WHEEL BRAKE FORCE AND WHEEL SPEED TIME TRACES FOR A MODULATING ANTI-SKID SYSTEM [MITCHELL, (1995)].....	31
FIGURE 14: IMPROVEMENT IN AIRCRAFT ANTI-SKID SYSTEM EFFICIENCY ON DRY RUNWAYS SINCE 1950 (SOURCE: CRANE SYSTEMS).	32
FIGURE 15: TYPICAL EFFICIENCY OF DIFFERENT ANTI-SKID SYSTEMS AS FUNCTION OF MAXIMUM FRICTION COEFFICIENT ([SAE, (2012), ATTRI & AMBERG, (1975), ATTRI ET. AL. (1974), ATTRI (1969), STRAUB ET. AL. (1974) AND TORENBEEK, (1982)].....	34
FIGURE 16: EXAMPLES OF VARIATION IN C-141 AIRCRAFT WHEEL BRAKE PRESSURE AND VELOCITY AND AIRCRAFT ACCELERATION DURING MAXIMUM BRAKING CONDITIONS ON DRY AND WET RUNWAYS [HORNE ET. AL. (1970)].....	35
FIGURE 17: COMPARISON OF ANTI-SKID EFFICIENCY OF A FULLY MODULATED SYSTEM ON DRY AND FLOODED RUNWAYS [YAGER AND MCCARTY (1977)].	36
FIGURE 18: EXAMPLE OF A MODERN ANTI-SKID SYSTEM (SOURCE: CRANE CO. HYDRO-AIRE INC., ANTISKID TUTORIAL)....	38
FIGURE 19: HYDROPLANING SPEEDS FOR DIFFERENT AIRCRAFT TYRES AS FUNCTION OF INFLATION PRESSURE (MAINLY OBTAINED FROM FULL SCALE AIRCRAFT TESTS).	40
FIGURE 20: INFLUENCE TYRE TREAD ON THE WATER FLOW UNDER TYRE FOOTPRINT (SOURCE: NASA TESTS).	42
FIGURE 21: ILLUSTRATION OF THE FLATTENING OF THE BOW WAVE WHEN REACHING OR EXCEEDING THE FULL (DYNAMIC) HYDROPLANING SPEED.	44
FIGURE 22: EXAMPLE OF MEASURED WHEEL SPEEDS ON A SLUSH COVERED RUNWAY FOR A CV880 AIRCRAFT (SOMMERS ET. AL. (1962)].....	45

FIGURE 23: EFFECTIVE BRAKING FRICTION COEFFICIENT AS FUNCTION OF GROUND SPEED FOR A RANGE OF AIRCRAFT ON FLOODED RUNWAYS.	50
FIGURE 24: EXAMPLE OF THE CONVAIR CV-880 TESTED IN A SPECIALLY PREPARED POND ON THE RUNWAY FILLED WITH SLUSH.	51
FIGURE 25: EFFECTIVE BRAKING FRICTION COEFFICIENT OF A SINGLE TYRE ON A FLOODED RUNWAY (SMOOTH SURFACES)....	53
FIGURE 26: PICTURE OF THE NASA AIRCRAFT LANDING DYNAMICS FACILITY WITH THE SLED WITH TEST TYRE BEING LAUNCHED (SOURCE: NASA).	54
FIGURE 27: COMPARISON OF SINGLE TYRE TESTS BRAKING FRICTION RESULTS WITH FULL SCALE B737-100 TESTS RESULTS ON A SMOOTH FLOODED RUNWAY.	55
FIGURE 28: MAXIMUM BRAKING FRICTION COEFFICIENT OF SINGLE TYRES ON A FLOODED RUNWAY.	56

LIST OF TABLES

TABLE 1: OVERVIEW OF THE GENERAL CHARACTERISTICS OF THE FRICTION DATA ON FLOODED RUNWAYS COLLECTED.....	48
---	----

1 INTRODUCTION

1.1. The Programme

FUTURE SKY SAFETY is an EU-funded transport research programme in the field of European aviation safety, with an estimated initial budget of about € 30 million, which brings together 32 European partners to develop new tools and new approaches to aeronautics safety, initially over a four-year period starting in January 2015. The first phase of the Programme research focuses on four main topics:

- Building ultra-resilient vehicles and improving the cabin safety
- Reducing risk of accidents
- Improving processes and technologies to achieve near-total control over the safety risks
- Improving safety performance under unexpected circumstances

The Programme will also help coordinate the research and innovation agendas of several countries and institutions, as well as create synergies with other EU initiatives in the field (e.g. [SESAR](#), [Clean Sky 2](#)). Future Sky Safety is set up with an expected duration of seven years, divided into two phases of which the first one of 4 years has been formally approved. The Programme has started on the 1st of January 2015.

FUTURE SKY SAFETY contributes to the EC Work Programme Topic MG.1.4-2014 Coordinated research and innovation actions targeting the highest levels of safety for European aviation, in Call/Area Mobility for Growth – Aviation of Horizon 2020 Societal Challenge Smart, Green and Integrated Transport. FUTURE SKY SAFETY addresses the Safety challenges of the ACARE Strategic Research and Innovation Agenda (SRIA).

1.2. Project context

Within the FUTURE SKY SAFETY programme the project *Solutions for runway excursions* (P3) was initiated to tackle the problem of runway excursions. A runway excursion is the event in which an aircraft veers off or overruns the runway surface during either take-off or landing. Safety statistics show that runway excursions are the most common type of accident reported annually, in the European region and worldwide. There are at least two runway excursions each week worldwide. Runway excursions are a persistent problem and their numbers have not decreased in more than 20 years. Runway excursions can result in loss of life and/or damage to aircraft, buildings or other items struck by the aircraft. Excursions are estimated to cost the global industry about \$900M every year. There have also been a number of fatal runway excursion accidents. These facts bring attention to the need to identify measures to prevent runway excursions.

Several studies were conducted on this topic. Most recently a EUROCONTROL sponsored research “Study of Runway Excursions from a European Perspective” showed that the causal and contributory factors leading to a runway excursion were the same in Europe as in other parts of the world. The study findings made extensive use of lessons from more than a thousand accident and incident reports. Those lessons were used to craft the recommendations contained in the European Action Plan for the Prevention of Runway Excursions, which was published in January 2013. This action plan is a deliverable of the European Aviation Safety Plan, Edition 2011-2014. The European Action Plan for the Prevention of Runway Excursions provides practical recommendations and guidance materials to reduce the number of runway excursions in Europe.

1.3. Research objectives

The Action Plan also identified areas where research is needed to further reduce runway excursion risk. The present project focuses on a number of these identified areas. Four areas of research were selected for which additional research is needed:

1. Research on the flight mechanics of runway ground operations on slippery runways under crosswind conditions;
2. Research on the impact of fluid contaminants of varying depth on aircraft stopping performance;
3. Research on advanced methods for analysis of flight data for runway excursion risk factors, and;
4. Research into new technologies to prevent excursions or the consequences of excursions.

The current report is written as part of topic number 2, task 3.2.1, “Description of the state of current knowledge regarding tyre braking performance, anti-skid systems, and modern aircraft tyres on water contaminated runways”. The objective of this task is to gain as much insight as possible on the braking capabilities of modern aircraft tyres on water contaminated runways.

1.4. Approach

Information and data mainly coming from public sources are used to describe the state of current knowledge regarding tyre braking performance, anti-skid systems, and modern aircraft tyres on water contaminated runways. Also data from older studies are considered as such data are often still the basis of the current knowledge and means of compliance used in aircraft performance analysis and certification.

1.5. Structure of the document

Section 2 of this report describes the factors that influence the braking friction capabilities of aircraft tyres on water contaminated runways. In section 3 aircraft anti-skid systems designs are discussed. Also their performance on slippery runways is discussed in this section. Section 4 deals with hydroplaning of modern aircraft tyres. In section 5 available data of aircraft braking on water contaminated runways are reviewed. Finally, section 6 gives the conclusions and recommendations.

2 BRAKING TRACTION OF AIRCRAFT TYRES ON WATER CONTAMINATED RUNWAYS

2.1. General introduction

The vast majority of takeoffs and landings are conducted on dry runways. Only a small portion is conducted on non-dry runways like water contaminated (flooded) runways¹ (see Figure 1). Statistics show that the likelihood of a runway excursion during takeoff or landing is much higher on flooded runways than on dry runways. Extreme loss of tyre braking can occur during rejected takeoffs and landings of aircraft on flooded runways. As a result the stopping distance increases significantly which could exceed the available runway length. The term hydroplaning, or aquaplaning, is used to describe this loss in traction on flooded runways. Hydroplaning is defined as the condition under which the tyre footprint is lifted off the runway surface by the action of the fluid. The forces from the fluid pressures balance the vertical loading on the wheel. Since fluids cannot develop shear forces of a magnitude comparable with the forces developed during dry tyre-runway contact, tyre traction under this condition drops to values significantly lower than on a dry runway. Water pressures developed on the surface of the tyre footprint and on the ground surface beneath the footprint originate from the effects of either fluid density and/or fluid viscosity, depending upon conditions. This has resulted in the classification of hydroplaning into two types, namely dynamic and viscous hydroplaning. Both types of hydroplaning can exist simultaneously and have the same impact on braking friction of the tyre. However, the factors influencing both types are different. This is discussed in more detail in the next sections.

¹ A runway can be considered flooded when more than 25 percent of the runway surface area (within the reported length and the width being used) is covered by water that is more than 3 mm in depth. This is then called a water contaminated runway or flooded runway.



Figure 1: Example of aircraft tyres braking on a very wet runway.

2.2. The 3-zone concept

To better understand the influence of both types of hydroplaning conditions, the contact surface of the tyre and the ground is divided into three zones, see e.g. [Moore, (1966); Horne, and Buhlmann (1983)]. Figure 2 illustrates the three zones under a tyre footprint of a braked or a free rolling tyre moving on a wet or flooded surface. In zone 1 the tyre contacts the stationary water film on the runway. The bulk volume of the water is being displaced in this zone. Zone 2 is a transition zone that consists of a thin water film. Finally zone 3 is a dry zone with no water film present between the tyre and the surface. Each zone in the footprint is discussed in more detail below.

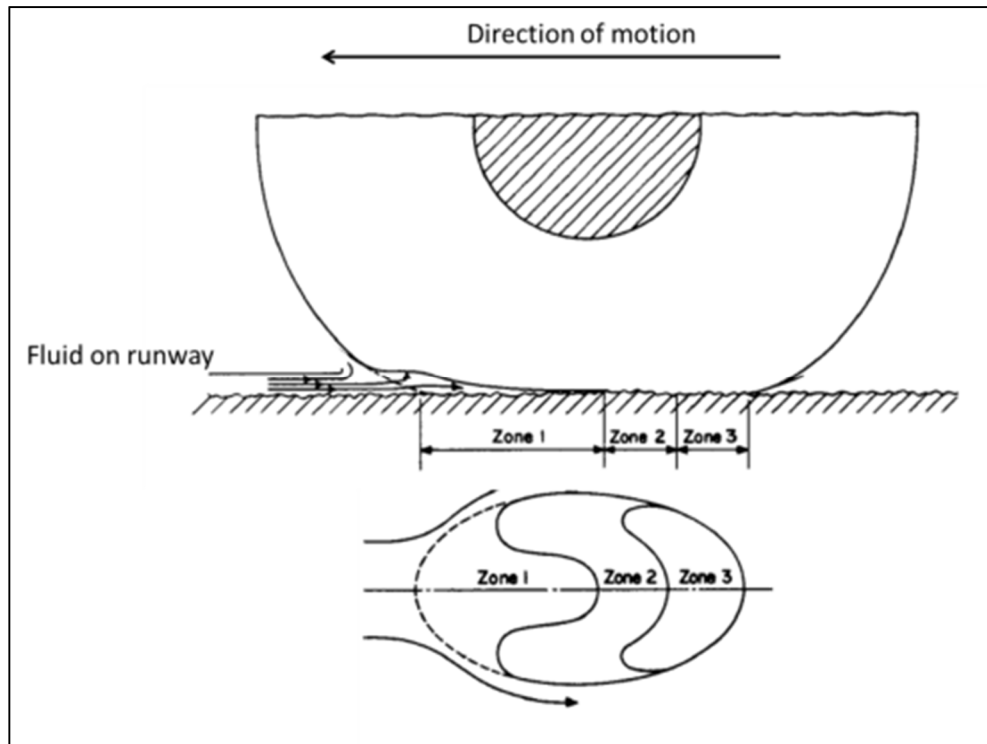


Figure 2: Zones under a tyre footprint when rolling along a wet/flooded surface.

In **zone 1** much of the water is ejected as spray and squeezed through the tyre's tread and the runway texture. Hydroplaning in zone 1 is the result of the hydrodynamic forces developed when a tyre rolls on a water covered surface. This is a direct consequence of the tyre impact with the water which overcomes the fluid inertia. The magnitude of the hydrodynamic force varies with the square of the tyre forward ground speed and with the density of the fluid [Horne and Upshur, (1965)]. The contact pressure developed between tyre tread and pavement establishes the escape velocity of bulk water drainage from beneath the footprint. Therefore high inflation pressure tyres can drain surface water more readily from the footprint than low inflation pressure tyres due to higher water escape velocities [I'Anson, (1973)]. With increasing ground speed zone 1 extends farther back into the contact area. At a certain (high) ground speed, zone 1 can extend throughout the contact area. Zone 2 & 3 then no longer exist and the tyre becomes completely detached from the ground, see e.g. [Niskanen and Tuononen, (2014)]. This is called full dynamic hydroplaning. The critical ground speed at which this condition occurs is referred to as the dynamic hydroplaning speed. When the condition of full dynamic hydroplaning is reached, the tyre stops rotating (spin-down). Dynamic hydroplaning is influenced by a number of factors like tyre inflation pressure, tyre tread, water depth and runway macrotexture, see e.g. [I'Anson, (1973)]. Macrotexture is the runway roughness formed by the large stones and/or grooves

in the surface of the runway (see illustration in Figure 4). The macrotexture provides escape channels to drain bulk water from zone 1. The drainage channels are provided by the tyre tread draping over the asperities of the pavement surface texture leaving valleys between the tyre tread and the low points of the surface texture through which bulk water can drain out from under the tyre footprint. The bulk water drainage through the macrotexture delays the build-up of fluid dynamic pressure to much higher speeds than the speeds found for pavements with no or little macrotexture. The tyre tread grooves in the tyre footprint are vented to atmosphere and provide escape channels for the bulk water trapped in zone 1. The tyre tread grooves act similar to the pavement macrotexture in draining the bulk water. When there is sufficient macrotexture on the surface and/or the tyre has a sufficient number of deep circumferential grooves, complete dynamic hydroplaning will normally not occur, unless the water depth is high enough so that both tyre grooves and runway macro texture cannot drain the water sufficiently quick enough.

Zone 2 is a transition region. There is only a thin film of water in this zone and water pressure is maintained by viscous effects (hence the name viscous hydroplaning). Viscous hydroplaning typically occurs on wet/flooded runways that have a smooth microtexture. Microtexture is the sandpaper like roughness of a surface formed by the sharpness of the fine grain particles on the individual stone particles of the surface (see illustration in Figure 4). Pavement microtexture performs its function by providing the surface a large number of sharp pointed projections that, when contacted by the tyre tread, generate very high local bearing pressures. This intense pressure quickly breaks down the thin water film and allows the tyre to regain dry contact with the pavement surface texture. Viscous hydroplaning can occur at ground speeds much lower than the speed for complete dynamic hydroplaning. Also the minimum water depth needed for viscous hydroplaning is much less than for dynamic hydroplaning [l'Anson, (1973)]. The pressure build-up in zone 2 is also much less dependent on ground speed compared to the pressure build-up in zone 1 [Horne and Upshur, (1965)]. Viscous hydroplaning is also not greatly affected by changes in tyre vertical load and tyre inflation pressure. In absence of zone 1 the area of zone 2 remains fairly constant through the speed range. For runways with a harsh microtexture, viscous hydroplaning is unlikely to occur as the microtexture penetrates and diffuses the thin water film. The area of zone 2 is relatively small or completely absent in this case. On runways with a smooth microtexture viscous hydroplaning can even occur on damp² surface conditions [Yager et. al. (1968)]. The fluid pressures developed in zone 2 between tyre and ground increases as the

² NASA considers a runway to be damp when there is 0 to 0.01 inches of water on the surface. In Europe a runway is considered to be damp when the surface is not dry, but when the moisture on it does not give it a shiny appearance.

fluid viscosity increases. The more viscous the fluid the more difficult it becomes for the tyre to squeeze the fluid from beneath the tyre and the surface. Therefore a high fluid viscosity enhances the possibility of viscous hydroplaning. When full viscous hydroplaning occurs, it is preceded by a wheel spin-down, see e.g. [l'Anson, (1973)]. As indicated a harsh microtexture is required to puncture and drain the viscous water film from the tyre/pavement interfaces that creates viscous water pressures beneath the tyre footprint in zone 2. However some additional thin film water drainage can be provided in zone 2 by tyre tread designs at the contact points between the pavement surface and tread rib. At these points, intense contact pressures are generated which can puncture and displace the water film in the same manner as the pavement surface microtexture. To be effective in draining the thin water film in zone 2, narrow slots or knife cuts in the rib surfaces are needed [Allbert and Walker, (1968); Danhof, (1981); Horne et. al (1965)]. Such rib designs are found on automobile tyres and not on commercial aircraft tyres due to tread chunking or tread retention problems [Horne, (1972)]. The tyres on commercial jet aircraft always have smooth rib surfaces and the tread patterns solely consist of circumferential grooves (see Figure 3). Circumferential grooves have a very small effect on removing the thin water film in zone 2. The effect is limited to the tread groove edges only. The actual depth of the circumferential grooves has no significant influence. In the end narrow slots or knife cuts in the rib surfaces are much more effective in draining the thin water film in zone 2 than circumferential grooves alone [Horne et. al (1965)]. It is sometimes suggested that grooved runways can alleviate viscous hydroplaning. However, similar to the circumferential grooves on the tyres themselves, the edges of the grooves in a runway are also not effective in providing pressures that can break down the thin water film.

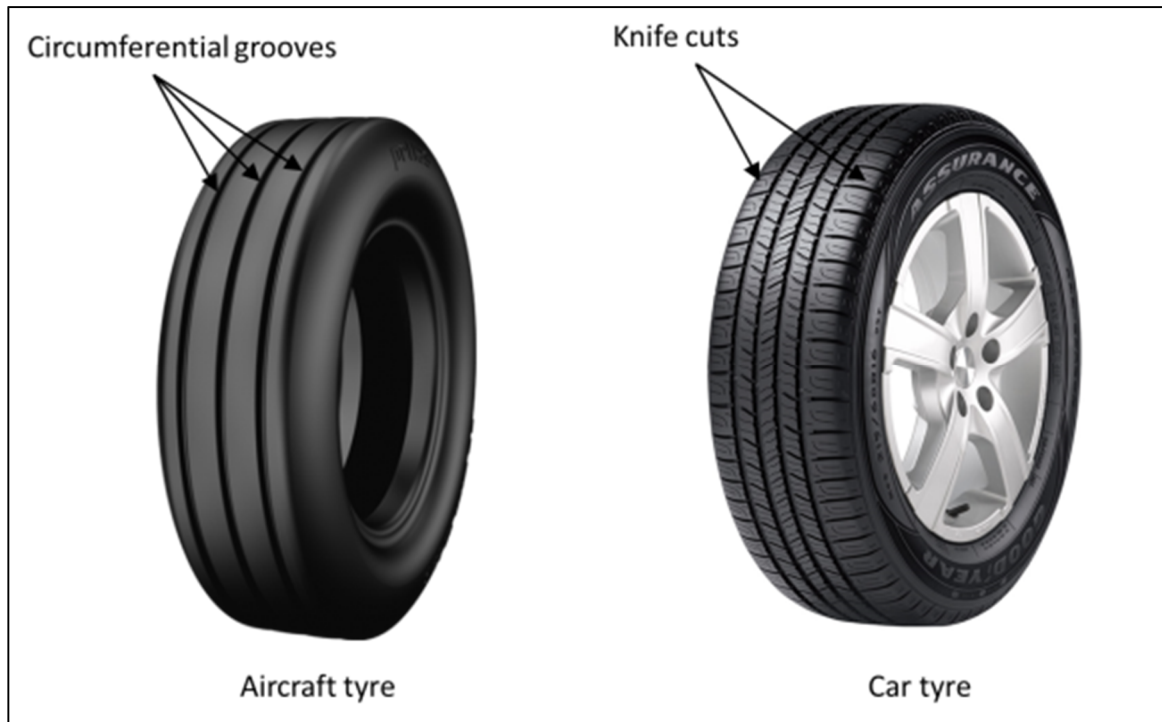


Figure 3: Tyre treads of aircraft and car tyres.

Zone 3 is a region of dry contact. The friction forces on the tyre are generated in this zone when the wheel is braked. The friction force is approximately equal to the dry runway friction force times the ratio of the contact area in zone 3 and the overall tyre-ground contact area [Horne and Buhlmann, (1983)]. Therefore the smaller zone 3 gets, the lower the braking friction forces become. When a tyre is fully separated by a film of water the braking friction coefficient³ for an aircraft tyre is very low as fluids cannot develop shear forces of a significant magnitude. Test data show that the braking friction coefficient on aircraft tyres can be less than 0.10 in this condition, see e.g. [Yager et. al (1990)]. On wet/flooded runways Zone 1 of the tyre-ground contact area may become so large at high speeds that contact between the tyre and the runway is lost. It is found that increasing inflation pressure tends to offset this effect as the dynamic hydroplaning speed increases with tyre pressure. This is in contrast to the effect that an increasing inflation pressure has on the braking friction forces in zone 3. Experimental data show that the *dry* runway braking friction coefficient decreases with increasing tyre inflation pressure[Balkwill (2015), Jones (2012)]. However this effect is smaller than the influence of the tyre pressure on the size of zone 1. In the classical literature the effect of vertical load changes on friction

³ Defined as the ratio of the friction force on the tyre and the tyre normal load.

coefficients on *dry* surfaces is assumed to be negligible since the tyre acts as an elastic body and the footprint area increases with the load with little change in tyre pressure. However, recent studies have shown a different result. Although the first law of friction states that the friction force is directly proportional to the vertical load, recent analysis showed that the vertical load can have an influence on the braking friction on an aircraft tyre sliding under heavy loading [Balkwill (2015), Jones (2012)]. Under light loading, as the vertical load is increased, the real area of contact increases proportionally to the vertical load. However, as the tyre becomes heavily loaded the valleys between the asperities begin to become filled. As the vertical load increases the real area of contact is no longer proportional to the vertical load. As a result the coefficient of friction decreases with increasing vertical load [Jones (2012)]. This then also applies to the frictions forces generated in zone 3.

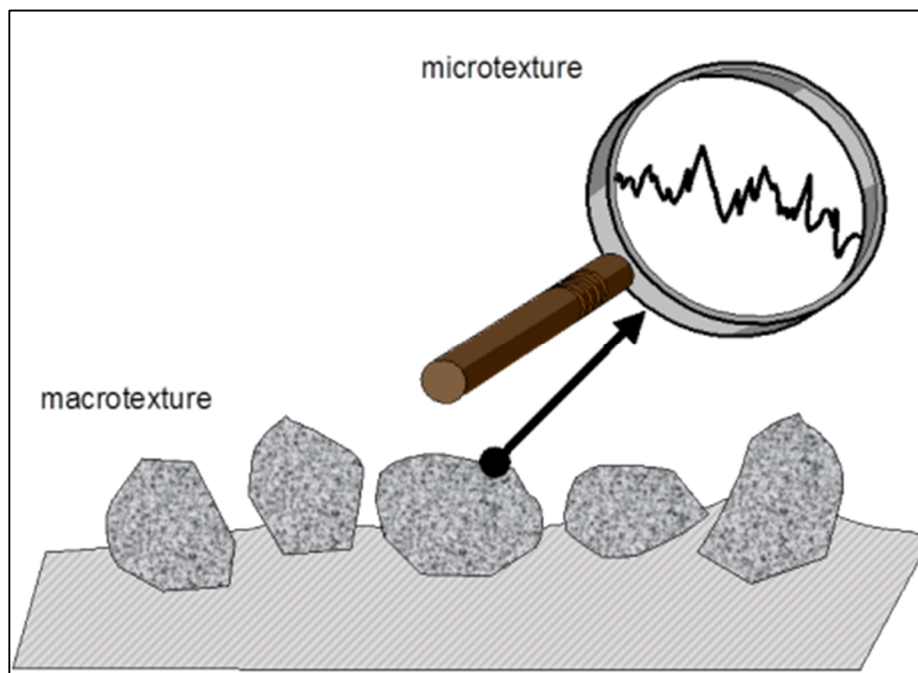


Figure 4: Illustration of macro- and microtexture on a runway surface [Van Es and Giesberts, (2003)].

2.3. Influence of runway macro- and microtexture on braking friction

On a wet/flooded surface the microtexture influences the tyre-runway braking friction starting from relatively low ground speeds and up where the runway macrotexture is mainly responsible for reducing friction at high speeds. These combined effects of runway texture are illustrated in Figure 5. The influence of the tyre-ground friction as function of ground speed is illustrated in this figure for different combinations of macro- and microtexture for both dry and wet surfaces. It is apparent that a pavement surface must possess both high macrotexture and a harsh microtexture to facilitate the relief of water trapped in the tyre/pavement contact zone in order to obtain good aircraft tyre traction during wet/flooded runway operations.

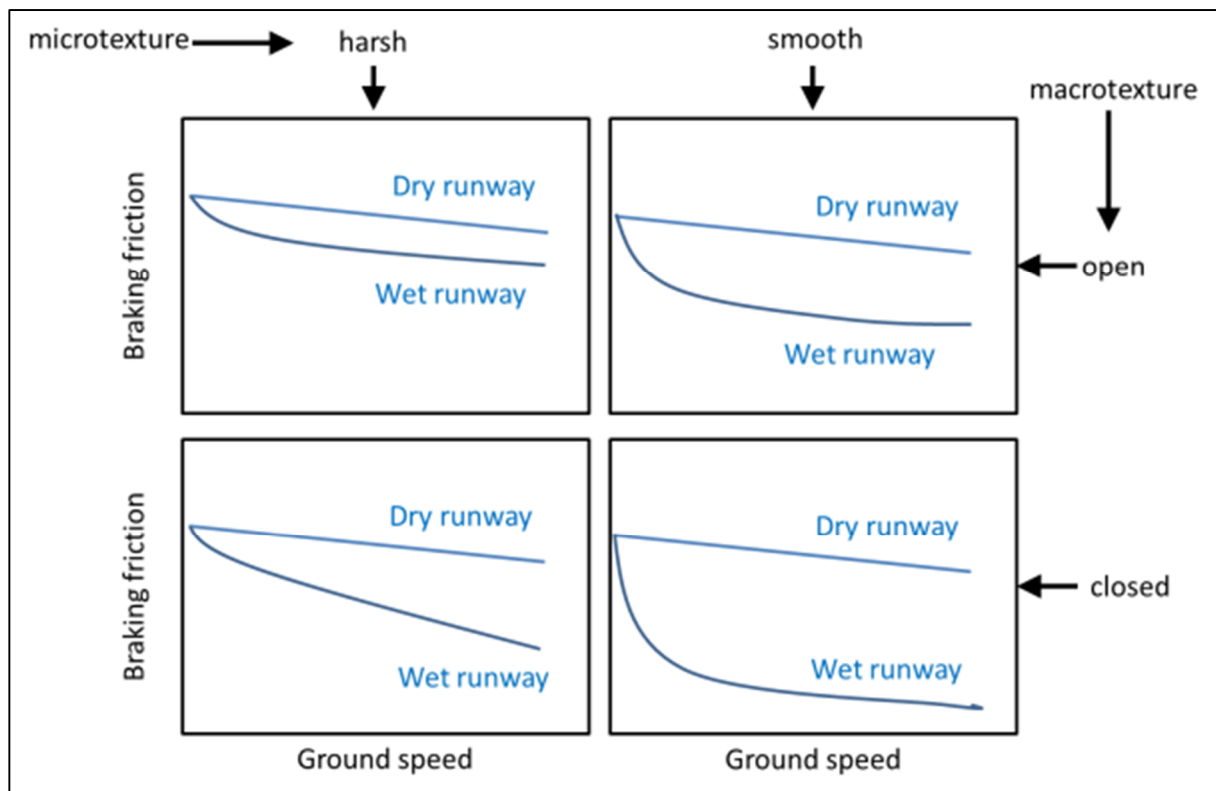


Figure 5: Influence of runway texture on tyre-ground braking friction as function of ground speed.

Although the physics of a braking tyre on a wet surface are similar to those on a flooded surface, the impact on the braking capability is normally much more significant on a flooded surface than on a wet surface because of the larger amount of water underneath the tyre footprint. This effect is most noticeable at high speeds when the dynamic pressure below the tyre surfaces is high and zone 1 becomes large. The size of zone 2 is much less depended on the water depth. Figure 6 illustrates the

braking friction coefficient as function of ground speed of a single tyre on dry, wet, and flooded surfaces. This clearly shows the large impact of a flooded surface on braking capabilities at high speeds. Figure 7 shows this same effect for a B737-100. Note that the low speed data for the dry runway conditions could be for the torque limited region of the brake system at which the braking force is kept constant. This results in a lower effective braking friction coefficient.

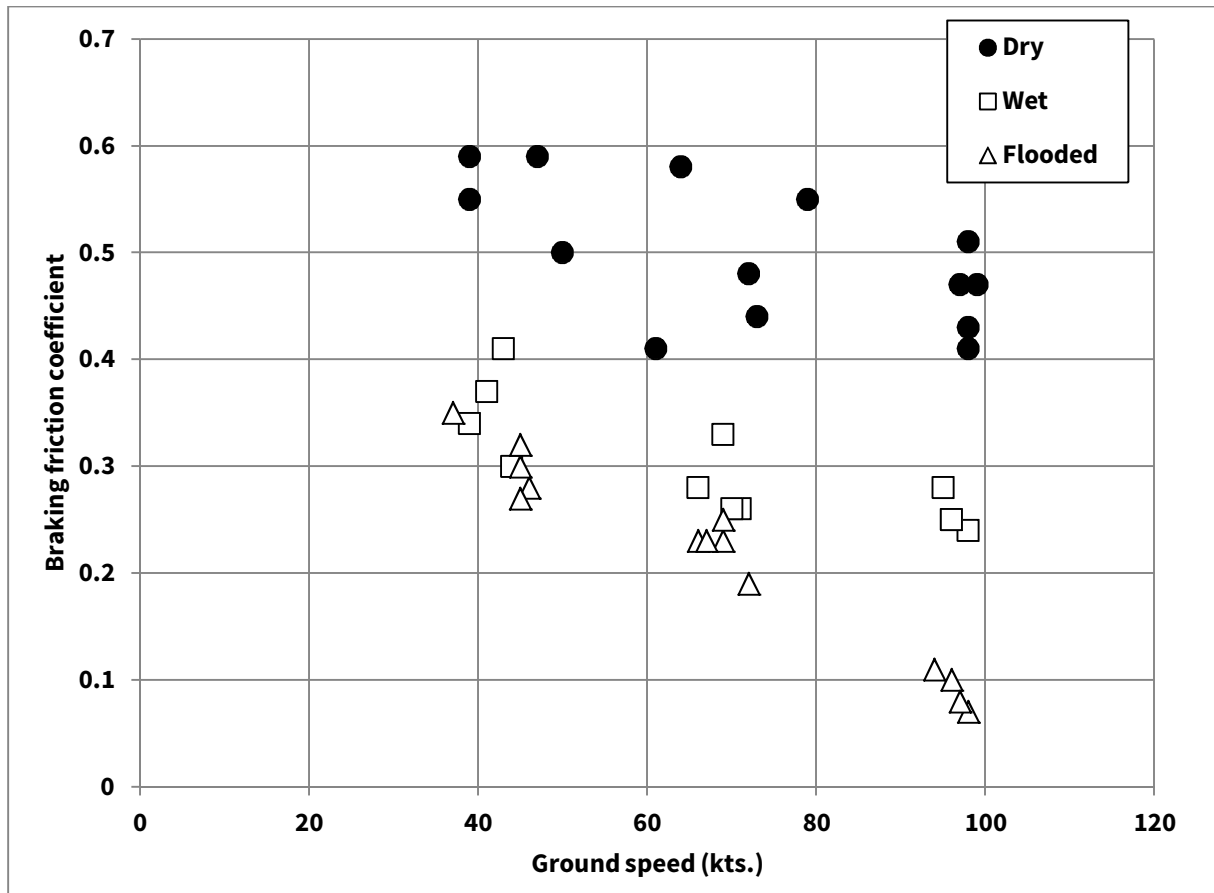


Figure 6: Comparison of the maximum braking friction coefficient as function of ground speed of a single tyre on a dry, wet, and flooded surface [Tanner et. al. (1981)].

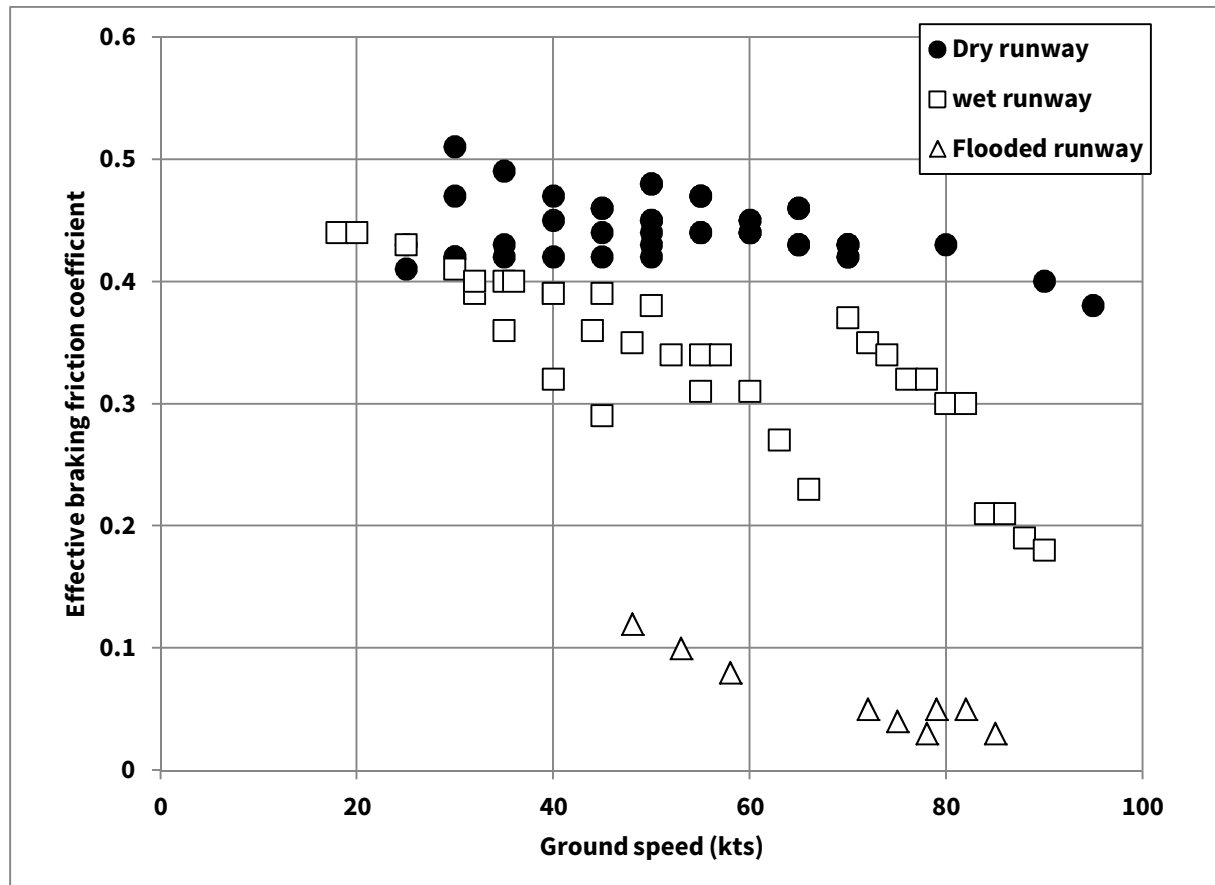


Figure 7: Comparison of the effective braking friction coefficient as function of ground speed on a dry, wet, and flooded runway for a B737-100 [Yager et. al. (1990)].

3 ANTI-SKID SYSTEMS

3.1. Introduction

When a brake torque is applied to a rolling tyre, the tyre circumferential speed is less than the forward speed. This speed differential arises as deformation and sliding of the tread material in the tyre-ground contact area. The overall effect is referred to as braking slip. When a rolling tyre is forced by a torque to slow rotation from a free-rolling condition, the friction coefficient developed between tyre and ground varies with the slip ratio. This relation is illustrated in Figure 8. The slip ratio is defined as the difference between the peripheral velocity of the wheel and the horizontal velocity of the wheel axle. The mechanics of force transfer from the tyre to the ground are provided by adhesion and hysteresis effects, for which 'slipping' of tyre tread elements in the contact area is needed. Slip is therefore needed to generate braking friction forces.

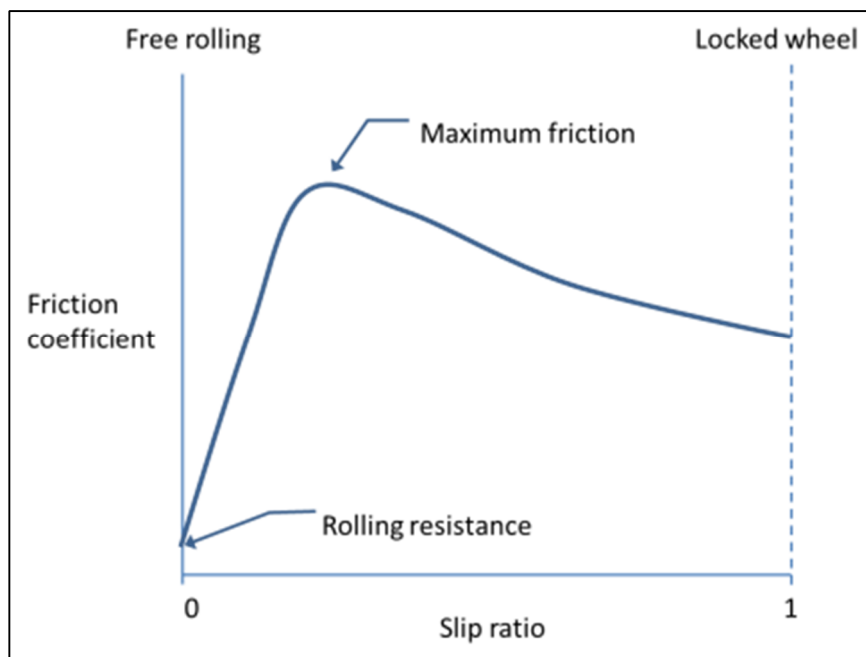


Figure 8: Relation braking friction and slip ratio [see e.g. Holmes (1970)].

The initial slope of the friction coefficient-slip curve (see Figure 8) is determined by the elasticity of the tyre. As illustrated in Figure 8 there is a slip ratio that gives the highest (peak) friction at which the

maximum numbers of tread elements produce maximum adhesion. In practice the braking friction coefficient-slip relation of a tyre is a function of a number of variables like runway condition, ground speed, and tyre temperature. For a wet or flooded surface the maximum friction coefficient reduces compared to a dry runway as discussed in the previous section. Runway condition also has an effect on the braking friction coefficient-slip relation as illustrated in Figure 9. Also the slip ratio at which maximum friction occurs can be different compared to a dry surface. Under flooded conditions, at speeds near full hydroplaning the braking friction coefficient-slip relation becomes more flat than for dry runways with a much less distinct slip ratio at which a peak in the friction can be observed.

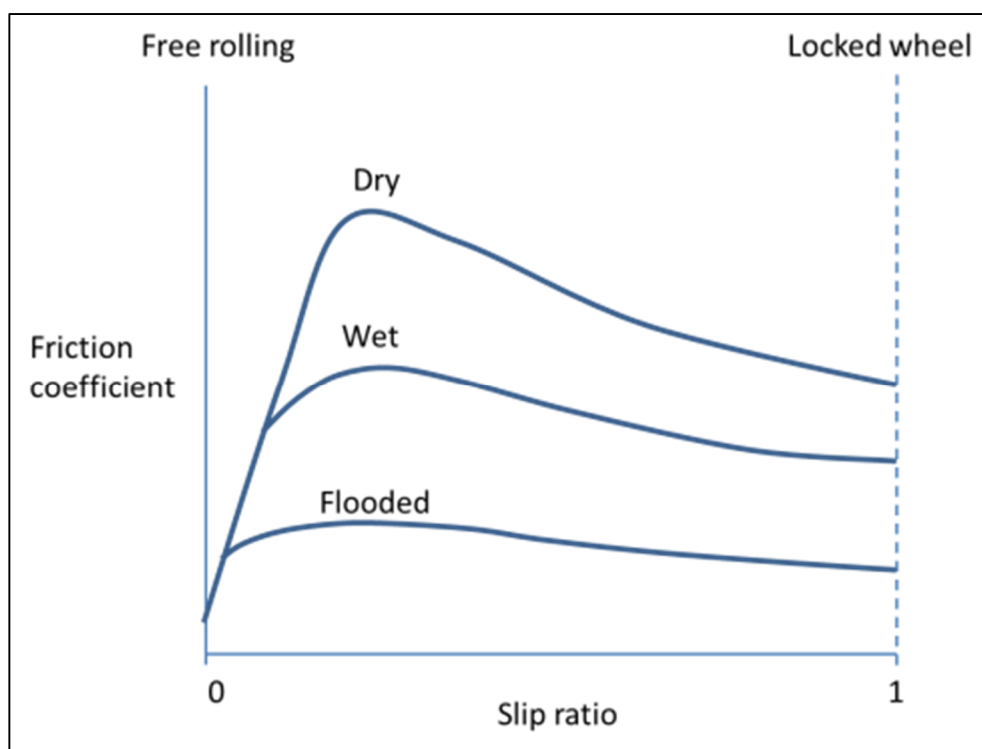


Figure 9: Illustration of influence of runway condition on μ slip ratio relation.

In general, it is not possible for a pilot to detect the reduction in braking friction when exceeding the optimum slip ratio. Thus if the brakes are manually controlled, it is difficult to obtain a consistent, high level of braking force and at the same time avoid possible burst or damaged tyres during periods of locked-wheel skidding. This becomes even more difficult on slippery runways. These problems have been overcome by the introduction of anti-skid systems in which brake control is achieved either by reference to wheel angular acceleration or to braking slip ratio.

The anti-skid system provides a means of detecting an incipient skid condition of the aircraft tyres and functions to control the brakes to maximise braking efficiency and avoid lock-up of the wheels. If a skid occurs the anti-skid system will release the brake pressure which allows the wheel to spin up again. The system then allows the brake effort to resume. This process is illustrated in Figure 10. A modern anti-skid system changes the brake clamping force to generate a brake torque such that the tyre runway friction force is maintained close to its peak value. If there are no incipient skids, the antiskid system does not interfere with the pilot brake pedal input. The anti-skid system can only override the pilot's input and command a reduction in the brake clamping force to stop the incipient skids when occurring.

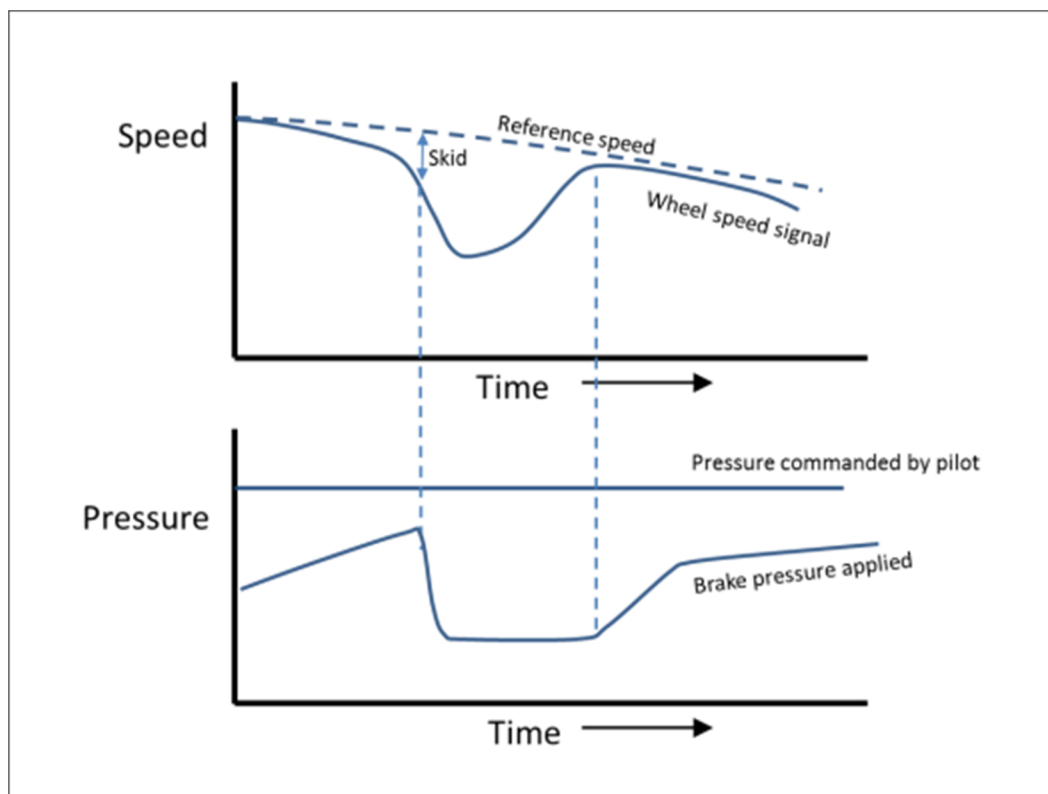


Figure 10: Illustration of the functioning of an anti-skid system [Elliot and DeVlieg (1978)].

Figure 11 shows a typical data trace from a flight data recorder of an aircraft (EMB-145) that landed on a flooded runway. Shown are a number of variables as function of time, including pilot brake pedal input and the anti-skid commanded brake pressures. Initially one pilot applied about half the maximum pedal input. Later both pilots applied braking and increased the pedal input to its maximum. However, as can be seen from the plots, the brake pressures do not increase following this maximum pedal input. The anti-skid is controlling the brake pressures being applied to the brakes of all four wheels by

reducing the commanded brake pressure to stop the incipient skids from occurring. The low, cycling braking pressures seen in Figure 11 are typical for a tyre braking on a slippery runway. Note that the flight data recorder stores the brakes pressure only once per second. Internally the system works at 200 Hz for this particular aircraft.

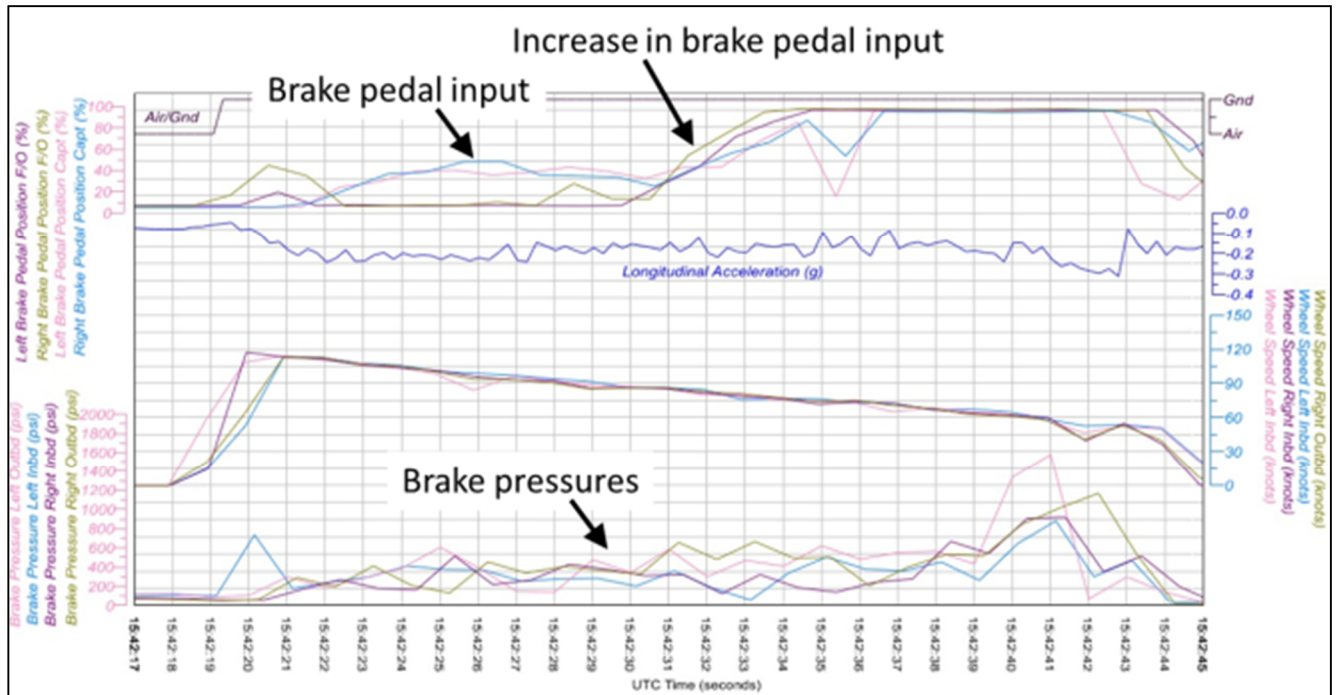


Figure 11: Example of an anti-skid working on a flooded runway (source: Colombia, Aeronautica Civil, Accident Report, ERJ-145 HK 4536, 2010).

3.2. Description of different anti-skid systems and their performance on slippery runways

Early anti-skid systems were based on the on-off control concept. These were designed primarily to prevent wheel locking and risk of tyre damage. The on-off systems exhibit a cyclic behaviour of brake pressure application until a skid is sensed, followed by the complete release of brake pressure to allow the wheel to spin back up. Full-metered pressure (as commanded by the pilot) is then re-applied, starting the cycle over again if another skid is entered. Figure 12 gives an example of wheel brake force and wheel speed time traces for an on-off anti-skid system. The size of the shaded area underneath the brake force graph is a measure for the efficiency of the anti-skid. Because of the large cycle behaviour of the on-off system this area is relatively small compared to the total area underneath the dashed line

plotted along the brake force peaks. This is an indicating of the low efficiency of the on-off anti-skid system.

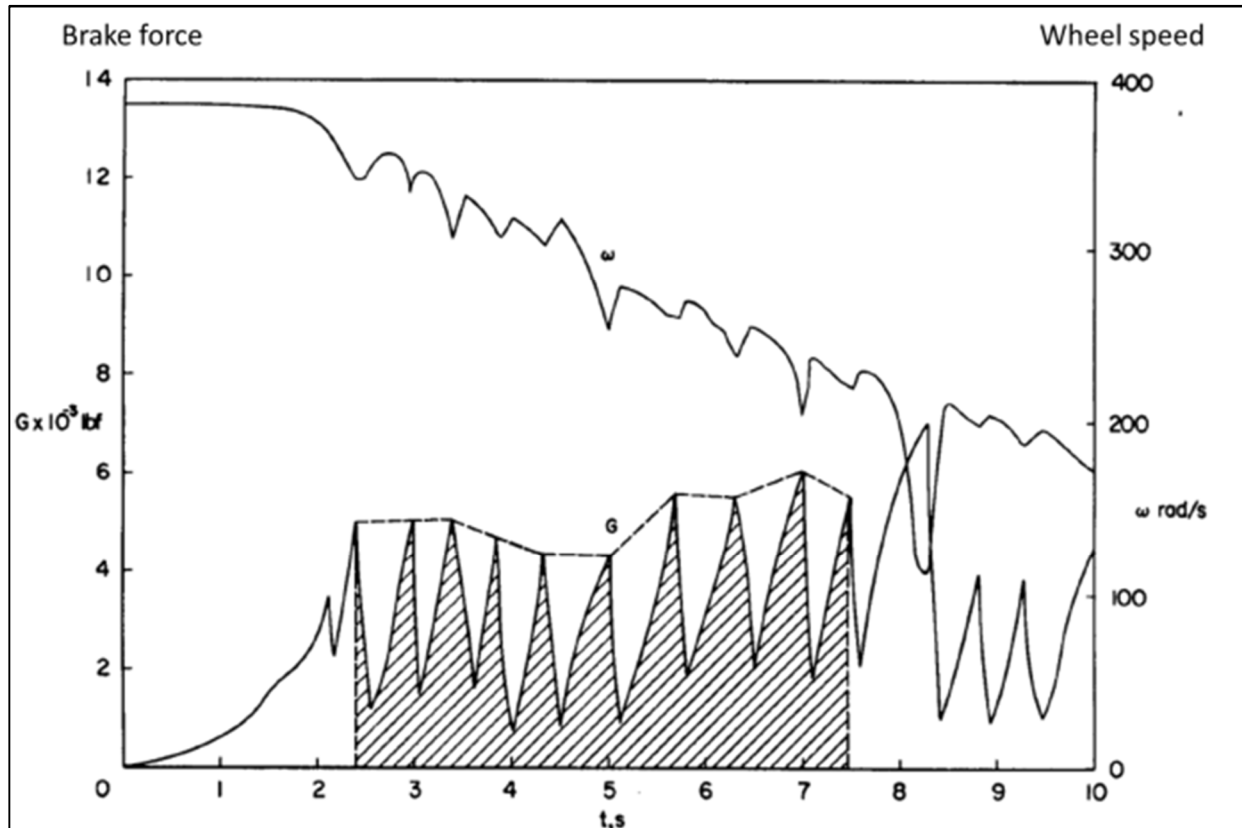


Figure 12: Example of wheel brake force and wheel speed time traces for an On-Off anti-skid system [Mitchell, (1995)].

After the introduction of on-off type anti-skid systems, it became apparent from various tests that braking effectiveness could be increased if the number of anti-skid cycles and their intensity could be minimised. A number of devices utilising various principles of operation have been used for this purpose. These devices predominately utilise the principle of "modulating" brake pressure to keep its value as near as possible to that which will produce a skid. It simply modulates the release and re-application of the brake pressure after entering a skid condition. Figure 13 gives an example of wheel brake force and wheel speed time traces for a modulating anti-skid system. Compared to the on-off system shown in Figure 12, the size of the shaded area underneath the brake force graph for the modulating system is much larger and closer to the area underneath the dashed line, meaning a more efficient system.

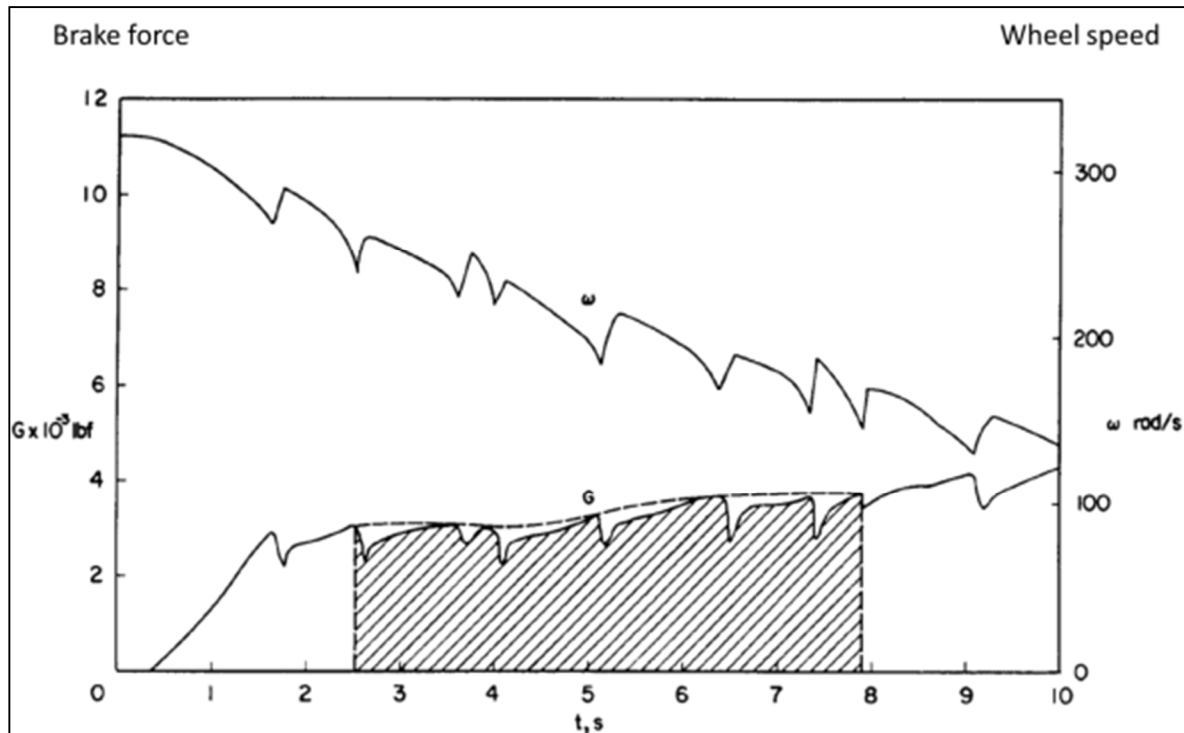


Figure 13: Example of wheel brake force and wheel speed time traces for a modulating anti-skid system [Mitchell, (1995)].

The first generation of modulating systems, released the brake pressure when the computed wheel deceleration exceeded a rate threshold value indicating an incipient skid (quasi-modulating systems). The corrective actions taken by these systems to exit the skid condition are based on a pre-programmed sequence. The difference between actual rate and the rate threshold is then used to reduce the brake pressure applied to the wheels. This is then followed by a wheel spin-up and re-applying of the brake pressure to a level below at which the skid was previously detected [Lester & Phil, (1973)]. The first generation of modulating systems provide a longer period over which a high proportion of the available runway friction is used than the on-off systems [Lester & Phil, (1973)].

Currently most transport aircraft have fully modulating anti-skid systems which differ from the quasi-modulating systems in the skid control logic. These systems are not based on the concept of rate threshold. During a skid, corrective action is based on the sensed wheel speed signal, rather than a pre-programmed response. The amount of pressure reduction or reapplication is based on the rate at which the wheel is going into or recovering from a skid. Full modulating systems have an advanced digital

control logic with high frequency wheel speed transducers, multiple data control functions and nonlinear computing elements.

Since the first introduction of anti-skid systems in the late 1940s the efficiency of these systems has improved significantly (see Figure 14). The ability of a skid control system to maintain control near the peak of the mu-slip curve is a measure of its efficiency. The efficiency is defined here by the ratio of the average friction coefficient and the maximum (peak) friction coefficient. The average friction coefficient is also called effective braking friction.

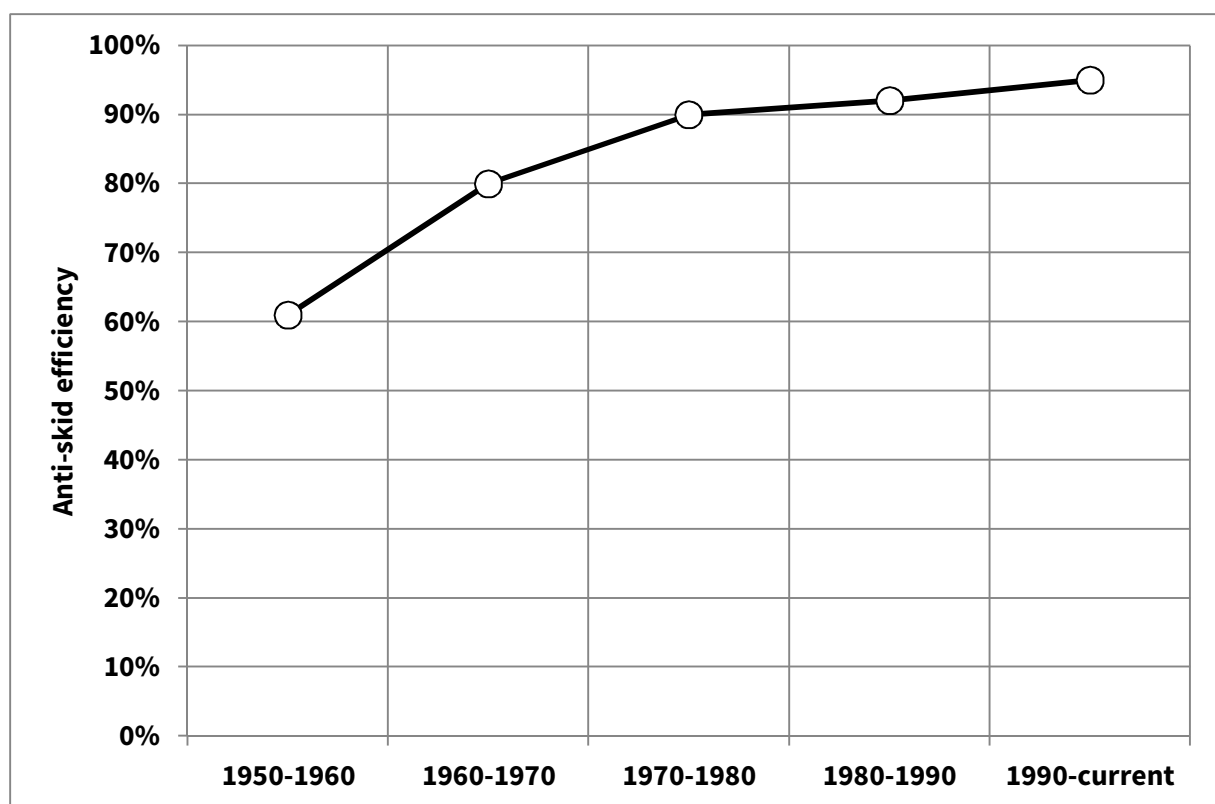


Figure 14: Improvement in aircraft anti-skid system efficiency on dry runways since 1950 (source: Crane Systems).

The braking efficiency that can be achieved depends on the design characteristics of the anti-skid. This is illustrated by Figure 15 which gives an example of the anti-skid efficiency of different designs as function the maximum friction coefficient of the surface-tyre combination. The low friction coefficients on slippery runways cause tyre spin-up accelerations to be lower than those on a dry surface. The reduced spin-up accelerations increase the time required for the tyre to recover from a deep skid and can lead to a degradation in anti-skid efficiency [Tanner (1982)]. On slippery runways the brake

pressure are significantly reduced in order to avoid deep skids. The response characteristics of some earlier anti-skid systems are diminished at these lower pressure levels thus leading to a lower braking efficiency of the anti-skid system [Tanner (1982)]. The anti-skid efficiency is also influenced by ground speed, normal load fluctuations, undercarriage vibration and suspension effects [Mitchel, (1995); Tanner (1972)]. Note that aircraft without anti-skid systems can only achieve a braking efficiency between 30%-50% through manual braking [Charman and Rekersdrees, (1974)].

As can be expected, on-off anti-skid systems have the lowest efficiency in obtaining the highest braking friction (see Figure 15). Under very low friction conditions the efficiency of these systems is further reduced by the low rate at which a wheel regains speed after the pressure has been released [Horne & Leland, (1962)].

The efficiency of quasi-modulating systems is much better than on-off systems. However the efficiency of quasi-modulating systems is also negatively influenced by the low tyre-surface braking friction. The efficiency is low for these systems on slippery surfaces such as a water contaminated runway. On dry runways, the quasi-modulating systems typically perform very well because the wheel speed recovers more quickly. A rapid re-application of brake pressure is then achieved with these systems. This is not the case when the surface is slippery. The fixed rate threshold used on quasi-modulating also does not work well on slippery surfaces as the rate threshold is based on dry runway deceleration. On a slippery runway this means that the braked wheel is entered a skid fairly deeply before action is taken by the antiskid system [Lester & Phil, (1973)] which reduces the efficiency of the anti-skid system.

Fully modulated anti-skid systems have the highest efficiency and are capable of exceeding 90% efficiency even on slippery runways as can be seen in Figure 15. Fully modulating systems show much smaller variations in brake pressure around the maximum value of friction. As a result, the average wheel speed remains much closer to the synchronous wheel speed, resulting in a high efficiency. Note that by regulation, the highest efficiency that can be claimed for a fully modulating antiskid system is 92%. However, higher efficiency values have been found during flight testing.

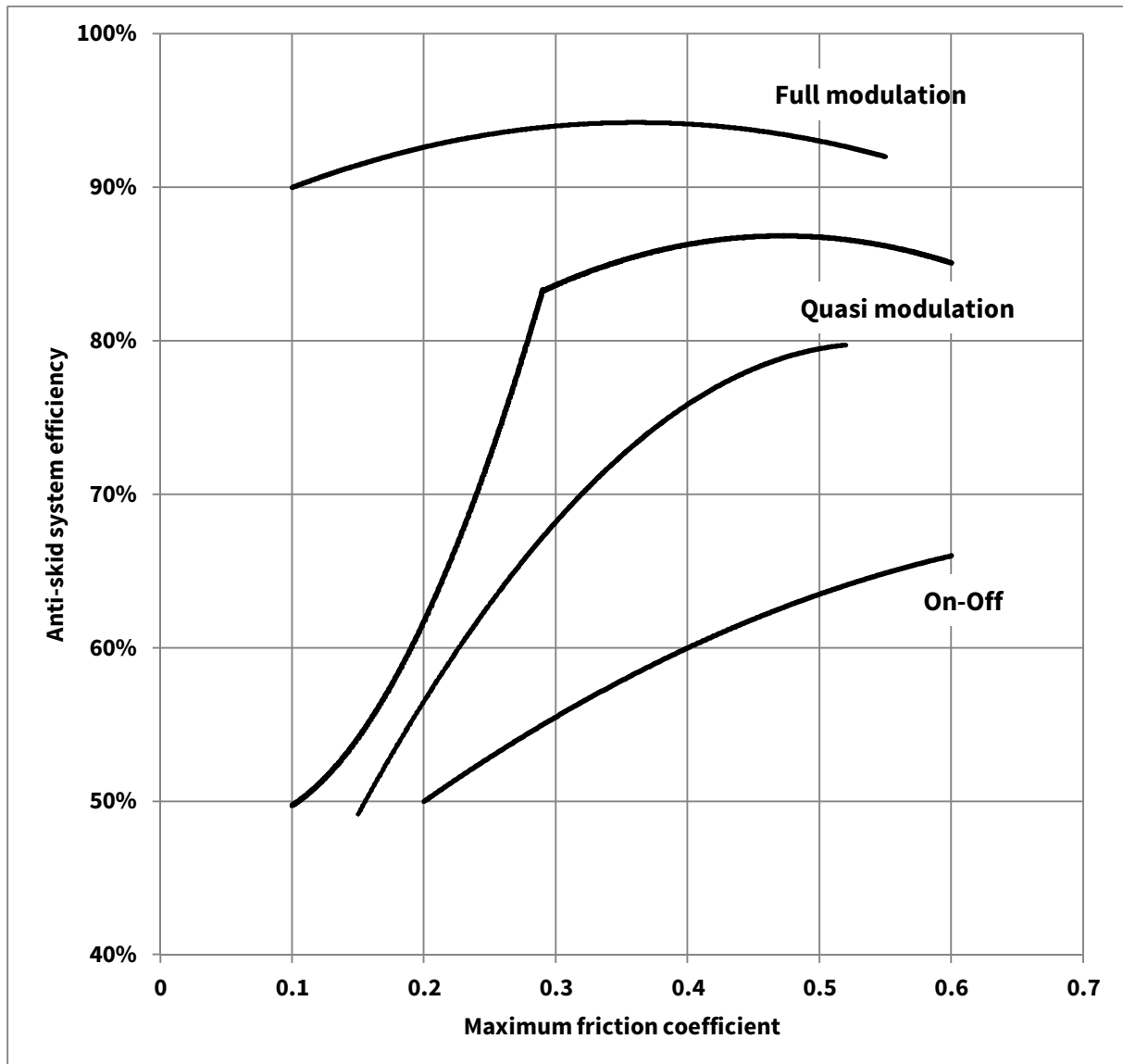


Figure 15: Typical efficiency of different anti-skid systems as function of maximum friction coefficient ([SAE, (2012), Attri & Amberg, (1975), Attri et. al. (1974), Attri (1969), Straub et. Al. (1974) and Torenbeek, (1982)].

The influence of runway slipperiness on the anti-skid performance is illustrated by some flight test data obtained with the C-141A aircraft in Figure 16. Examples of variation in C-141A aircraft wheel brake pressure and velocity and aircraft acceleration during maximum braking conditions on dry and wet runways are shown in Figure 16. The C-141A was equipped with a modulating anti-skid system. The influence of the runway condition on the anti-skid functioning is clearly visible from Figure 16. It can be seen that the anti-skid cycling increased from 1/2 cycle per second for the dry runway to 3.5 cycles per second for the wet runway.

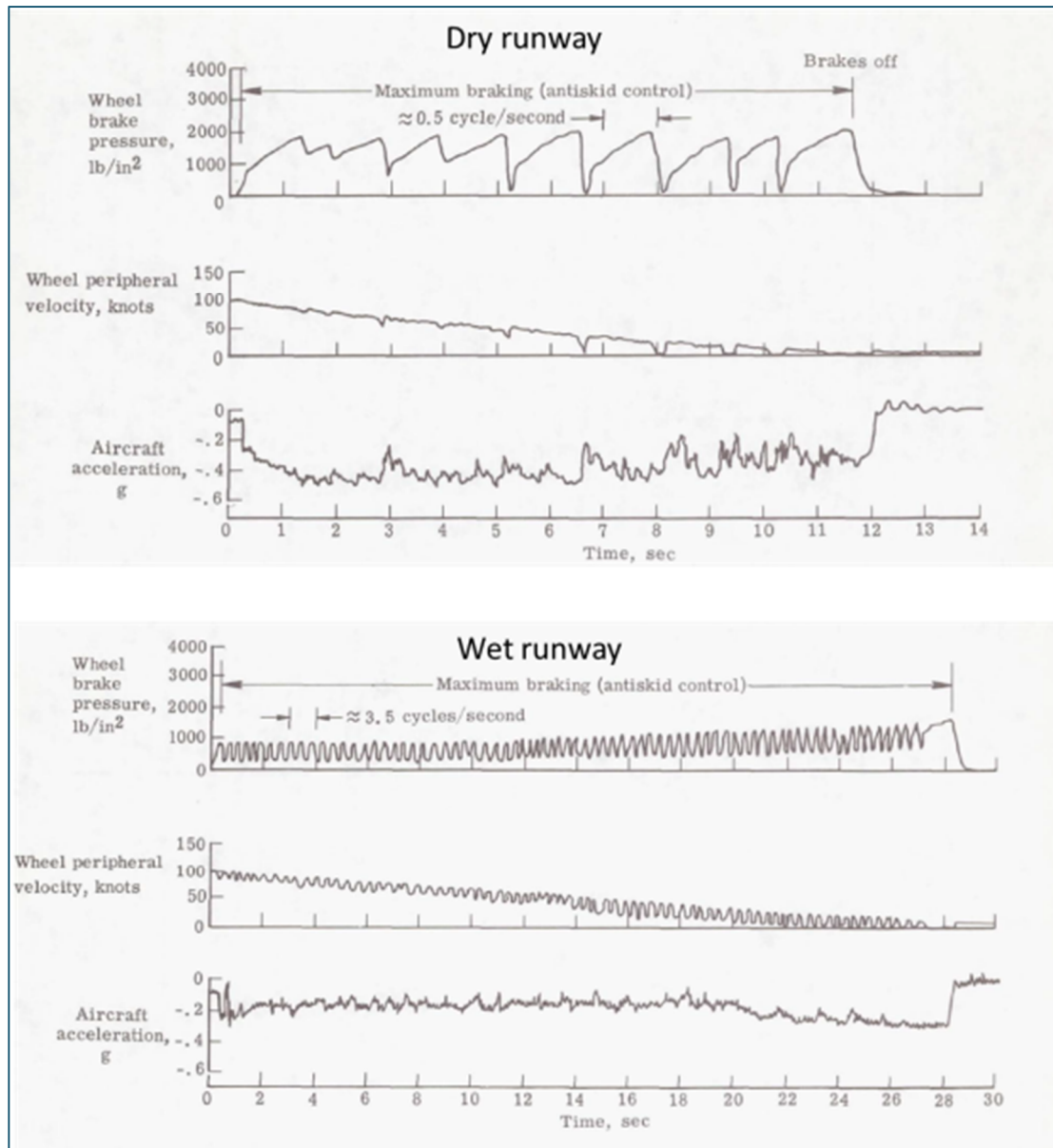


Figure 16: Examples of variation in C-141 aircraft wheel brake pressure and velocity and aircraft acceleration during maximum braking conditions on dry and wet runways [Horne et. al. (1970)].

Figure 17 gives an example of the anti-skid efficiency of a fully modulating system as function of ground speed for a dry runway and a flooded runway. On the dry runway the average efficiency was 89% and on the flooded runway this was somewhat less, namely 80%. In this example the antiskid system is a late 1970s design which performs somewhat better on a dry runway than on a slippery runway.

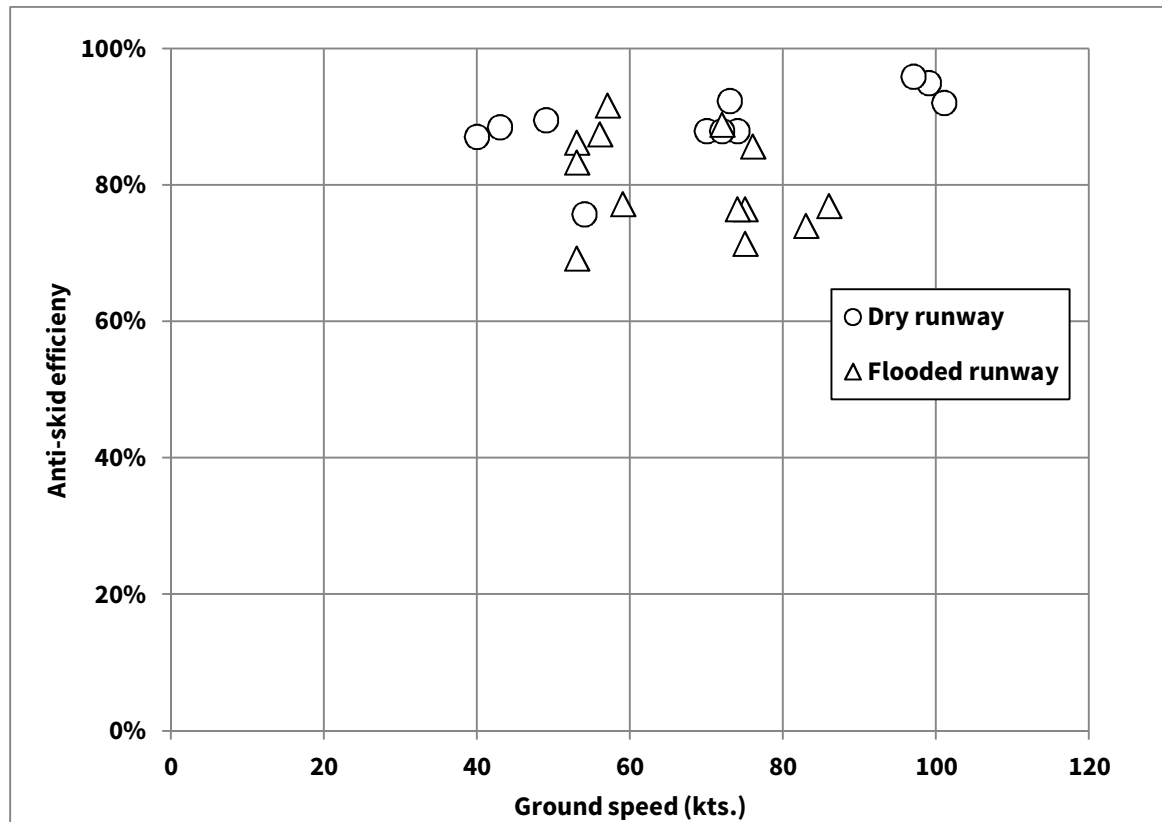


Figure 17: Comparison of anti-skid efficiency of a fully modulated system on dry and flooded runways [Yager and Mccarty (1977)].

3.3. Modern anti-skid design characteristics

Modern anti-skid designs have benefitted from computer simulations wherein tyre and brake data extracted from dynamometer testing, are combined with the properties of the aircraft landing gear to evaluate stopping performance for different runway conditions. While anti-skid systems are generally tailored for each aircraft application, many similarities exist as far as the basic design is concerned. A modern anti-skid system design is illustrated in Figure 18. This example is for a system designed by Crane Co. Hydro-Aire Inc. and is typical of the modern anti-skid designs currently used on commercial aircraft. The wheel speed signal is input to the anti-skid control unit where it is processed to produce a wheel velocity signal. The wheel velocity signal initialises a reference speed when “slip” speed is zero (no braking force applied) e.g. right after touchdown and full spin-up. The subsequent difference between wheel speed and reference speed is the speed error (e), which contains slip speed information. The reference speed is initially established when the wheels spin-up at touchdown and is then

continuously updated each time the wheels recover from a skid. In any event, the anti-skid system cannot function without a reference speed. The speed error signal (e) is input to three control elements:

- The pressure bias modulation function which is a time integral of error ($K_e dt$) that produces a slowly changing average pressure level to maintain brake pressure at a level that maintains slip near the optimum level;
- The transient control function (K_e) which provides a rapid and large scale adjustment to brake pressure when the velocity error is too large (onset of excess slip), and;
- The phase compensation function ($K de/dt$) which provides a small-signal compensation for brake system hydraulic phase-lag.

The anti-skid controls the amount of hydraulic pressure applied by the pilots on the brakes. If necessary the anti-skid system will reduce the metered brake pressure. The anti-skid is only active if the pilot meters a pressure in excess of that required to skid the tyre. The anti-skid does not apply pressure on the brakes, but only relieves it. This whole process is conducted at a very high frequency (typically 200 Hz), allowing the anti-skid to react quickly to changes in runway slipperiness.

When brakes are applied during severe tyre hydroplaning, the anti-skid system may lose its reference speed as the wheels are not spun up. The wheels remain locked up until the pilot releases the brake pedals. On some aircraft this problem is solved by using the groundspeed signals from the aircraft's inertial reference system as a backup wheel reference speed.

Modern antiskid systems also provide additional safety features like a touchdown protection and locked wheel protection.

The touchdown protection prevents landing with brake pressure applied to the brakes. This prevents that the wheels cannot spin-up at touchdown which is necessary for the anti-skid to function. Brake actuation will be normally allowed only after a number of seconds after touchdown or after the wheels have spun-up to a pre-set value.

The locked wheel protection prevents wheels from locking up during the ground roll. For this the anti-skid system compares wheel speeds signals between. If one wheel speed is say 30-50% lower than that of another wheel, a full brake pressure release is commanded to the associated wheel, allowing wheel

BRAKE PEDAL

SYSTEM HYDRAULIC PRESSURE

METERING VALVE

METERED PRESSURE

ANTISKID VALVE

ANTISKID PRESSURE

VELOCITY REFERENCE

VELOCITY ERROR

WHEEL VELOCITY

ANTISKID CONTROL UNIT

Ke

$\int Ke dt$

$K \frac{de}{dt}$

DOWNLOCK BUNGEE SPRINGS

SHOCK STRUT

WHEEL & TIRE

BOGIE BEAM

AXLE AXLE NUT

ANTISKID WHEELSPEED TRANSDUCER HUBCAP

WHEELSPEED TRANSDUCER

⁴ The actual speed difference varies amongst the different aircraft designs.

4 DYNAMIC HYDROPLANING OF MODERN AIRCRAFT TYRES

As discussed earlier dynamic hydroplaning plays an important role in the reduction of braking capabilities on flooded runways. On well-maintained runways the microtexture is such (harsh) that the contribution of viscous hydroplaning to the reduction of braking capabilities of a tyre is very small. However there are examples of runway excursions in which this was not the case and viscous hydroplaning occurred even during moderate rainfall. These runway excursions were solely caused by the poor maintenance of the runway. For wet/flooded runway braking performance analysis it is normally assumed that the runway has a harsh microtexture such that the viscous pressures below the tyre footprint in zone 2 are alleviated. Dynamic hydroplaning is then mainly responsible for the low braking friction on flooded runways.

Dynamic hydroplaning is the result of the hydrodynamic forces developed when a tyre rolls on a water covered surface. This is a direct consequence of the tyre impact with the water that overcomes the fluid inertia. The magnitude of the hydrodynamic force varies with the square of the tyre forward ground speed and with the density of the fluid (dynamic pressure). Dynamic hydroplaning is also influenced by tyre tread, water layer thickness and runway macrotexture. When there is sufficient macrotexture on the surface and / or the tyre has proper tread, total dynamic hydroplaning will usually not occur. However, hydroplaning can occur when the water depth is high enough so that both tyre tread and runway macro texture cannot drain the water quickly enough.

It has been found that modern aircraft tyres typically hydroplane at lower ground speeds than assumed earlier. Studies by NASA showed [Horne et. al., (1968)] that on a well flooded runway aircraft tyres typically started to experience a full dynamic hydroplane condition when the forward speed equals nine times the square root of the tyre inflation pressure. However later studies showed that this empirical equation does not apply to more recent tyre designs. This is illustrated in Figure 19, which shows experimental dynamic hydroplaning speeds obtained from full-scale tests for different aircraft tyre types under wide range of conditions (e.g. macrotexture depths, normal loads, water depths, and tyre groove depths). Basically all modern tyres shown in the figure have dynamic hydroplane speeds (well) below $9\sqrt{p}$ (in kts, with p the tyre inflation pressure in psi).

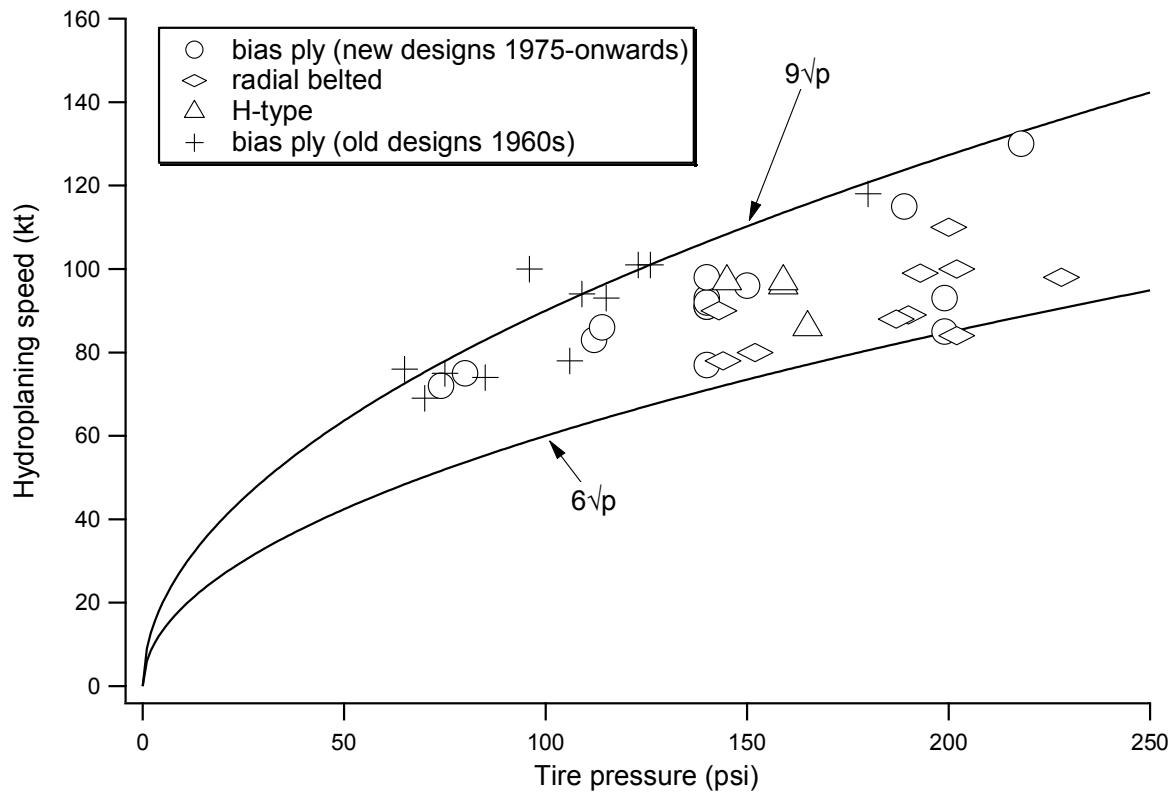


Figure 19: Hydroplaning speeds for different aircraft tyres as function of inflation pressure (mainly obtained from full scale aircraft tests).

To understand why modern aircraft tyres have a lower full dynamic hydroplaning speeds than older bias ply tyre designs (e.g. from the 60's), a model for full dynamic hydroplaning is discussed here.

The dynamic lift L generated under a tyre rolling along a fluid-covered surface is given by [Dreher et. al., (1963)]:

$$L = \frac{1}{2} \rho V^2 S C_{Lh} \quad (1)$$

with ρ the density of the fluid, S the tyre footprint area, V the ground speed and C_{Lh} the hydrodynamic lift coefficient. When total dynamic hydroplaning occurs, L/S is equal to the tyre bearing pressure that can be approximated by the tyre inflation pressure (p).

During full dynamic hydroplaning the tyre footprint is completely supported by a fluid film over a length L_f (footprint length). Considering a tread element on the surface of the tyre, the time (t) which the tread element needs to penetrate the fluid film completely, is given by [Bathelt, (1973); Schmit (1985)]:

$$t = \frac{L_f}{V_p} \quad (2)$$

It can be shown that t is a function of tyre pressure p , fluid density ρ and footprint width W_f [Bathelt, (1973); Bathelt, (1971); Schmit (1985)]:

$$t \cong W_f \sqrt{\frac{\rho}{p}} \quad (3)$$

Combining Eq. 2 and 3 results in a relation for the full dynamic hydroplaning speed:

$$V_p = \lambda \frac{L_f}{W_f} \sqrt{\frac{p}{\rho}} \quad (4)$$

where λ is a factor that depends on the surface macrotexture, tread of the tyre and water depth (see [Bathelt, (1973)] for details). It follows directly from Eq. 4 that the longer and the narrower the footprint is, the higher the dynamic hydroplaning speed becomes. The ratio of footprint length and width depends on the tyre construction, tyre size, tyre inflation pressure and vertical load. For instance increasing the vertical load will reduce the ratio of footprint length and width. For those cases where the water depth is roughly greater than the depth of tyre grooves and surface macrotexture texture depth, λ can be considered as an overall constant [Van Es, (2001)]. In case of a rolling tyre (either braked or unbraked) λ equals to a value of approximately 1 under these conditions. For a tyre that needs to spin-up after touchdown on a flooded surface, the constant λ is equal to approximately 0.85 [Van Es, (2001)]. Bulk water drainage and alleviation of dynamic water pressures in the tyre/ground contact zone are controlled by the runway surface macrotexture and tyre tread groove design (e.g. number of grooves and their width & depth). The water underneath the tyre is drained by the macrotexture and/or the tyre tread grooves, as such it reduces the pressure build up. This effect depends on the macrotexture depth, number of grooves in the tyre tread and the size (width and depth) of these grooves. These factors will influence the factor λ [Bathelt, (1973)]. The influence of circumferential grooves on the water flow in the tyre footprint is illustrated in Figure 20. The factor λ can be calculated by the methods provided in [Bathelt, (1973); Bathelt, (1971), Schmit (1985)], when the water depth is less than the sum of the macrotexture and tyre groove depth.

From static load tests it follows that the tyre footprint aspect ratio L_f/W_f of modern tyres is lower than for older designs of bias ply tyres of the same size and under equal conditions (pressure and vertical load). It follows directly from equation 4 that the full dynamic hydroplaning speeds will then be lower for these modern tyres. Also in the event of partial dynamic hydroplaning, zone 1 will be larger for modern tyres than for older cross-ply designs. The tyre footprint aspect ratio of modern cross-ply tyres compared to radial, and H-type⁵ tyres also differ from each other resulting in different dynamic hydroplaning speeds under the same conditions. The limited available wet runway braking tests do not show a large difference between these tyres [Yager, et. al. (1992); Yager, et. al. (1990)]. However, these NASA tests were conducted on very smooth runways with a macrotexture texture depth of only 0.13 mm and a water depth of less than 3 mm. This low texture depth could have a more dominate effect on the formation of zone 1 than the tyre footprint aspect ratio. Also the low water depth in combination with the grooved test tyres will reduce the size of zone 1 in the footprint. Differences were found in the cornering characteristics of these tyres under wet conditions [Yager, et. al. (1992); Yager, et. al. (1990); and Alsobrook (1987)]. Comparison of braking friction-slip behaviour of aircraft radial and cross ply tyres has revealed very similar initial slope and peak values under both wet and dry conditions [Alsobrook (1987)]. No braking tests data for flooded conditions are publicly available for both radial and H-type aircraft tyres.

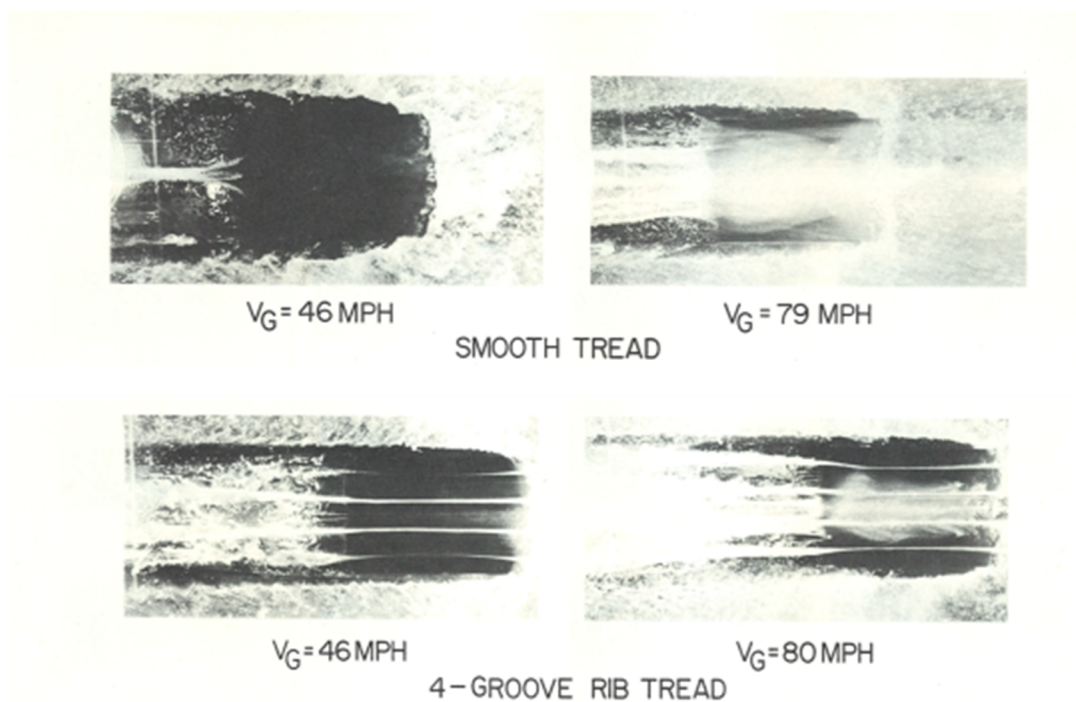


Figure 20: Influence tyre tread on the water flow under tyre footprint (Source: NASA tests).

⁵ The “H” identifies that the bias ply tyre is designed for a higher percent deflection. H type tyres also have a different rim width to tyre section ratio and a different taper.

The classic NASA formula for predicting the full dynamic hydroplaning speed under spin-down conditions, $9\sqrt{p}$, over-predicts the hydroplaning speed for modern aircraft tyres. This was already anticipated by some aircraft manufacturers which used a modified version of the classical dynamic hydroplaning equation for performance calculations during the late 70s. Following the simple NASA relation the available full scale experimental data suggest (see Figure 19) that a modern bias ply tyre would hydroplane (dynamically) on a flooded runway at around $8\sqrt{p}$, a H-type tyre around $7.5\sqrt{p}$ and a radial tyre around $6.9\sqrt{p}$, with the speed in knots and p in psi. These relations can be used for a rapid estimation of the spin-down dynamic hydroplaning speed in absence of experimental data. For landing (spin-up) no experimental data for modern aircraft tyres are available. A reduction of the spin-down dynamic hydroplaning speed of 15% could be used as a first estimate. This factor is based on older NASA tests [Joyner and Horne (1971)].

It must be noted that some of the scatter in the data shown in Figure 19 could be the result of the lack of consistent definitions for identifying the full hydroplaning speed from experimental data. There are several manifestations of (dynamic) hydroplaning that can be observed from test data: tyre bow wave suppression; water contamination drag peaks; and tyre spin-down. Experiments have shown a progressive reduction of the bow wave spray angle as ground speed increases. Above the hydroplaning speed bow wave flattens or disappears completely (see Figure 21). Around and above the hydroplaning speed the water displaced by the tyre is reduced significantly which results in a reduction of the fluid dynamic displacement drag on the tyre. A peak in the fluid contaminant drag can be observed around the hydroplaning speed. The strongest indication of dynamic hydroplaning is the condition of the wheels slowing down or stopping completely. The fluid dynamic lift force under the tyre causes the centre of pressure of the vertical ground reaction to move ahead of the wheel axle with increasing ground speed. This causes a spin-down moment. Near the hydroplaning speed this spin-down moment exceeds the total spin-up moment caused by all tyre drag forces. The tyre will then start to spin-down and can come to a complete stop. Above the hydroplaning speed the centre of pressure of vertical ground reaction moves back to wheel axle which causes the wheel to spin-up again (see Figure 22).

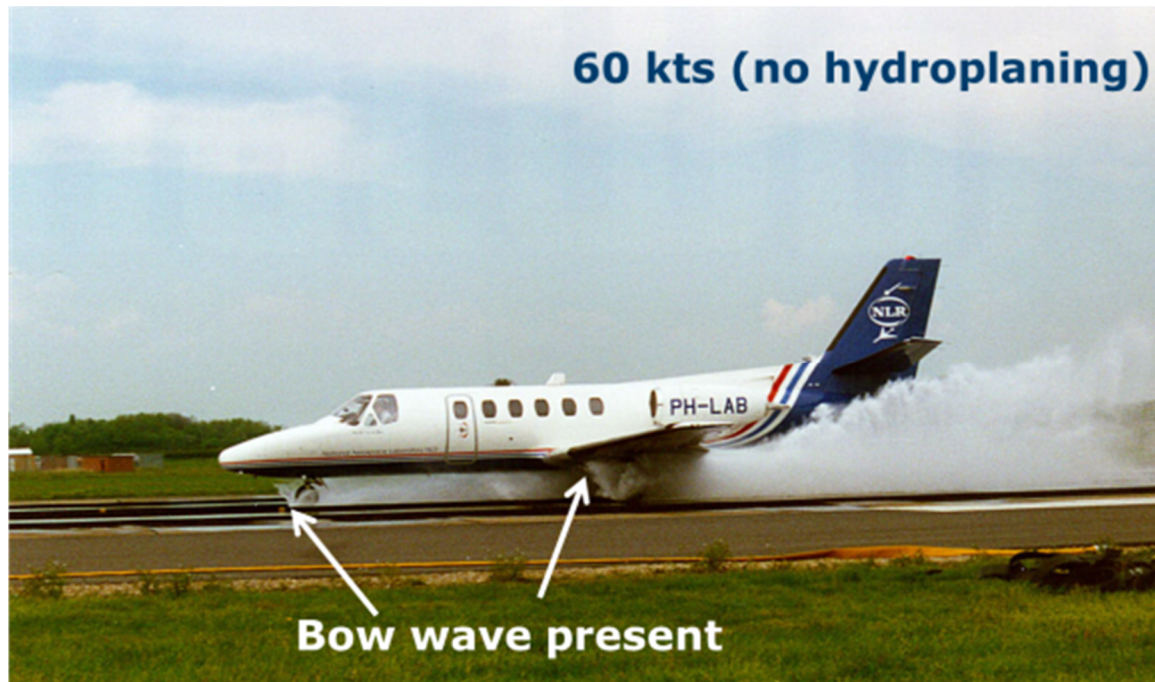


Figure 21: Illustration of the flattening of the bow wave when reaching or exceeding the full (dynamic) hydroplaning speed.

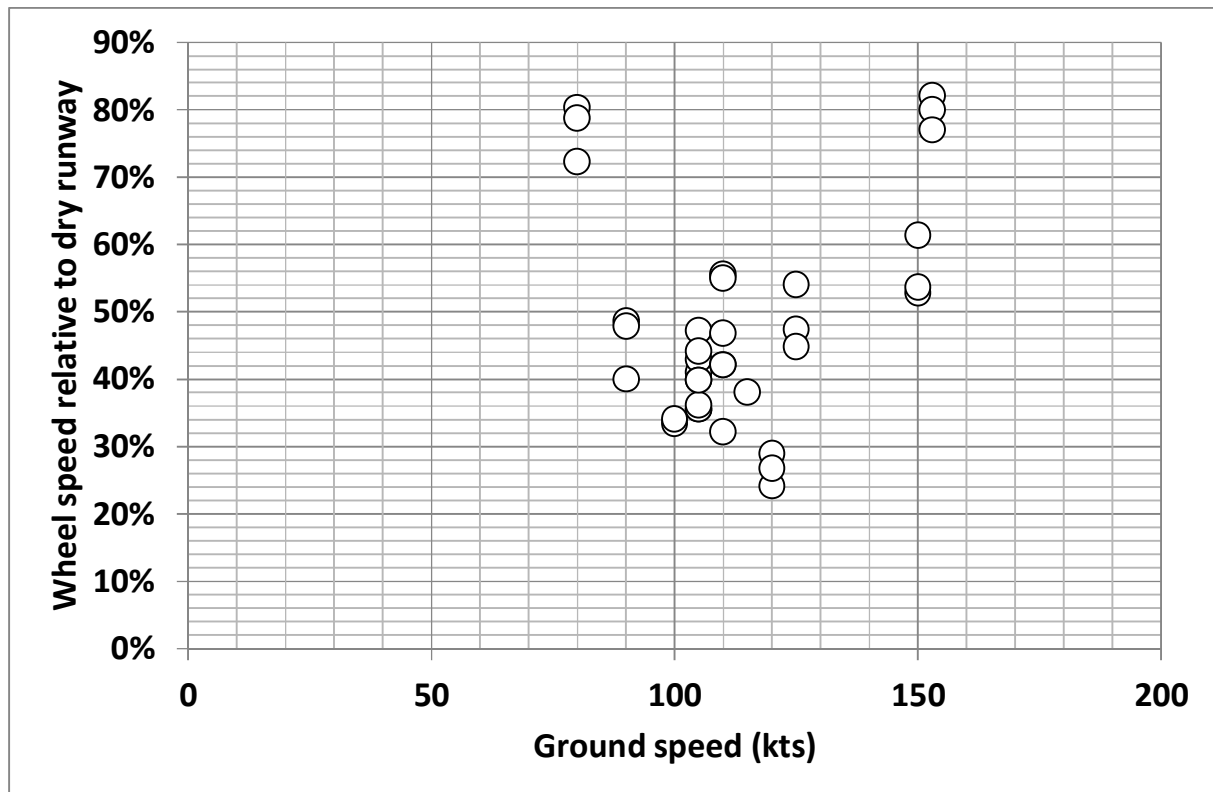


Figure 22: Example of measured wheel speeds on a slush covered runway for a CV880 aircraft (Sommers et. al. (1962)).

5 REVIEW OF EXPERIMENTAL DATA ON BRAKING CAPABILITIES OF AIRCRAFT TYRES ON FLOODED RUNWAYS

5.1. Data sources

In this section a review of available test data on braking capabilities of aircraft tyres on flooded runways is presented. These data are obtained from a wide variety of public sources. They originate from both aircraft tests as well as from full-scale traction facilities. The full-scale traction facilities often included an anti-skid device. These traction data facilities are comparable to some of the data obtained with full-scale aircraft. The basic data are formed by the combinations of ground speed and braking friction coefficient. Additional background data like water depth, tyre dimensions, texture depth etc. are also collected and are put into a database to be used for further analysis. The final database encompasses 409 data points (e.g. combinations of friction coefficient and ground speed).

Note that a runway is considered to be flooded if the water depth is 3 mm or more. However in many tests the water depth levels were not constant and varied along the track, sometimes below a value of 3 mm. This is unavoidable even on specially prepared surfaces that are almost level. The average water depth levels were measured on top of the surface asperities.

Table 1 provides an overview of some of the general characteristics of the data collected. Friction data on flooded runways were found for eight transport aircraft. All of these aircraft except the EMB145 are of old design and are no longer in production. Except for the Queen Air (tyre Type III⁶, manual braking) and the C-123B (tyre Type III, On-Off anti-skid), all these aircraft were equipped with a modulating anti-skid system and type VII bias ply tyres. The B737-100 in the data sample had a fully modulated (MKIII) anti-skid system installed. The EMB-145 had the most modern anti-skid which is part of a brake-by-wire system. The data for the EMB-145 are obtained from an accident investigation rather than a dedicated flight test. All other data were obtained through dedicated flight tests.

⁶ Type III tyres are generally used for low pressure service providing a larger footprint. Type III tyres have smaller rim diameters relative to the overall diameter as compared to other type designs. Speeds are generally limited to 160 mph or less.

The database also contains data from single tyre tests obtained from full-scale traction facilities (Type VII and VIII bias ply)⁷. Some of these tests were conducted with an anti-skid system installed and are therefore representative for full scale aircraft braking performance. Others were tested for a range of slip ratios and only the maximum friction coefficient was recorded in the present database. Most of the tyres in the single tyre tests had inflation pressures of 140 to 170 psi which is representative for the majority of commercial transport aircraft currently being operated. Also the tyre size matches with those found on many transport aircraft.

⁷ Type VII is known as the "extra high pressure" tyre. Section widths are generally narrower than other types. Type VIII was the last category to be identified as a type. It is considered to be "low profile-extra high pressure". It has a similar inflation pressure range to Type VII tyres.

Table 1: Overview of the general characteristics of the friction data on flooded runways collected.

Source	Aircraft type	Tyre type	Tyre Size	Tyre inflation pressure (psi)	Anti-skid type	Ground speed range (kts)
Yager, et. al (1990)	B727-100	VII bias ply	49 x 17-26	145	Quasi Modulated	25-55
Yager, et. al (1990)	B737-100	VII bias ply	40 x 14-24	155	Fully modulated	32-95
Horne et. al. (1970)	C141	VII bias ply	44 x16 -28	110	Quasi modulated	20-80
Shrager (1962)	CV880	VII bias ply	39 x 13 -22	155	Quasi modulated	10-95
Horne et. al. (1970)	CV990	VII bias ply	41x15-18	160	Quasi modulated	20-140
Yager et. al. (1971)	Queen Air	III bias ply	8.50 X 10	47	Manual braking	21-99
Sawyer and Kolnick (1959)	C123B	III bias ply	49 x 17 -16	65	On-Off	60-105
Baker (2011)	EMB-145	VII bias ply	19.5 X 6.75	145	Fully modulated	40-125
Stubbs and Tanner (1977)	Single tyre tests	VII bias ply	40 x 14 -22	140	Quasi modulated	45-103
Dreher et. al. (1974)	Single tyre tests	VIII bias ply	30 x 11.5- 14.5	265	None	5-98
Stubbs (1979)	Single tyre tests	VII bias ply	40 x 14-22	140	Fully modulated	52-104
Yager and Mccarty (1977)	Single tyre tests	VIII bias ply	30 x 11.5-14.5	265	None	5-97
Yager and Dreher (1976)	Single tyre tests	VIII bias ply	30x 11.5-14.5	265	None	5-100
Daiutole and Grisel (1981)	Single tyre tests	VII bias ply	49 x17-26	170	None	69-128
Agrawal and Daiutolo (1981)	Single tyre tests	VII bias ply	49 x17-26	140	None	70-140
Tanner et. al. (1981)	Single tyre tests	VII bias ply	40 x 14-22	140	Fully modulated	37-96
Agrawal (1983)	Single tyre tests	VII bias ply	49 xx17-26	140	None	33-149
Stubbs and Tanner (1976)	Single tyre tests	VII bias ply	40 x 14-22	140	Quasi modulated	47-99

5.2. Short analysis of available data

5.2.1. Full-scale aircraft tests

Figure 23 shows the effective braking friction coefficient as function of ground speed for a range of aircraft on flooded runways. These tests were conducted on smooth runways (macrotexture depths of less than 0.4 mm), on textured runways (macrotexture depth 0.4 mm or higher) and on grooved runways (with equivalent macrotexture depths higher than 1.5 mm). The water depths varied between 4-13 mm in these full-scale tests. The majority of the full scale tests were conducted on specially prepared sections of a runway. Water or slush⁸ was put on the runway and in order to maintain the required fluid depth, dikes made of rubber strips were put around the test section. An example of such a test is shown in Figure 24.

All tests except those conducted with the CV-880 and the B727-100 were conducted on water contaminated runways. For the CV-880 and B727-100 tests a slush covered runway was used. Although the density of slush is less than for water, its general impact on braking friction is more or less similar as above some level of water content, slush acts like a water. However, friction levels can be different due to the lower density of slush resulting in higher dynamic hydroplaning speed than on a water covered surface. In line with hydrodynamic theory, the full dynamic hydroplaning speed is an inverse function of the fluid density. This has been confirmed by test data on slush covered surfaces. Test data also showed that increasing fluid viscosity increases the fluid pressures developed between tyre and ground at a given speed. This will enhance the possibility of viscous hydroplaning on a slush covered runway. The traction loss at low speeds (where dynamic hydroplaning is not dominant) is much greater on the more viscous slush than on the water-covered runways. This can only be countered by a harsh microtextured runway. There is no information available on the microtexture of the runway on which the tests with the CV-880 took place⁹. The B727-100 tests were conducted on a textured runway with a harsh microtexture.

Figure 23 shows the effective braking friction coefficient measured at different ground speeds for number of transport aircraft. The differences in friction values at a given ground speed are caused by several factors like tyre pressure, runway texture, and fluid depth. All data show a significant decrease of the braking friction with increasing ground speed due to the increase of the dynamic pressures underneath the footprint of the tyres.

⁸ Slush is water-saturated snow having a liquid water content greater than 15%.

⁹ It is believed that the CV-880 tests were conducted on a moderately textured concrete runway (See AIAA paper No. 65-749).

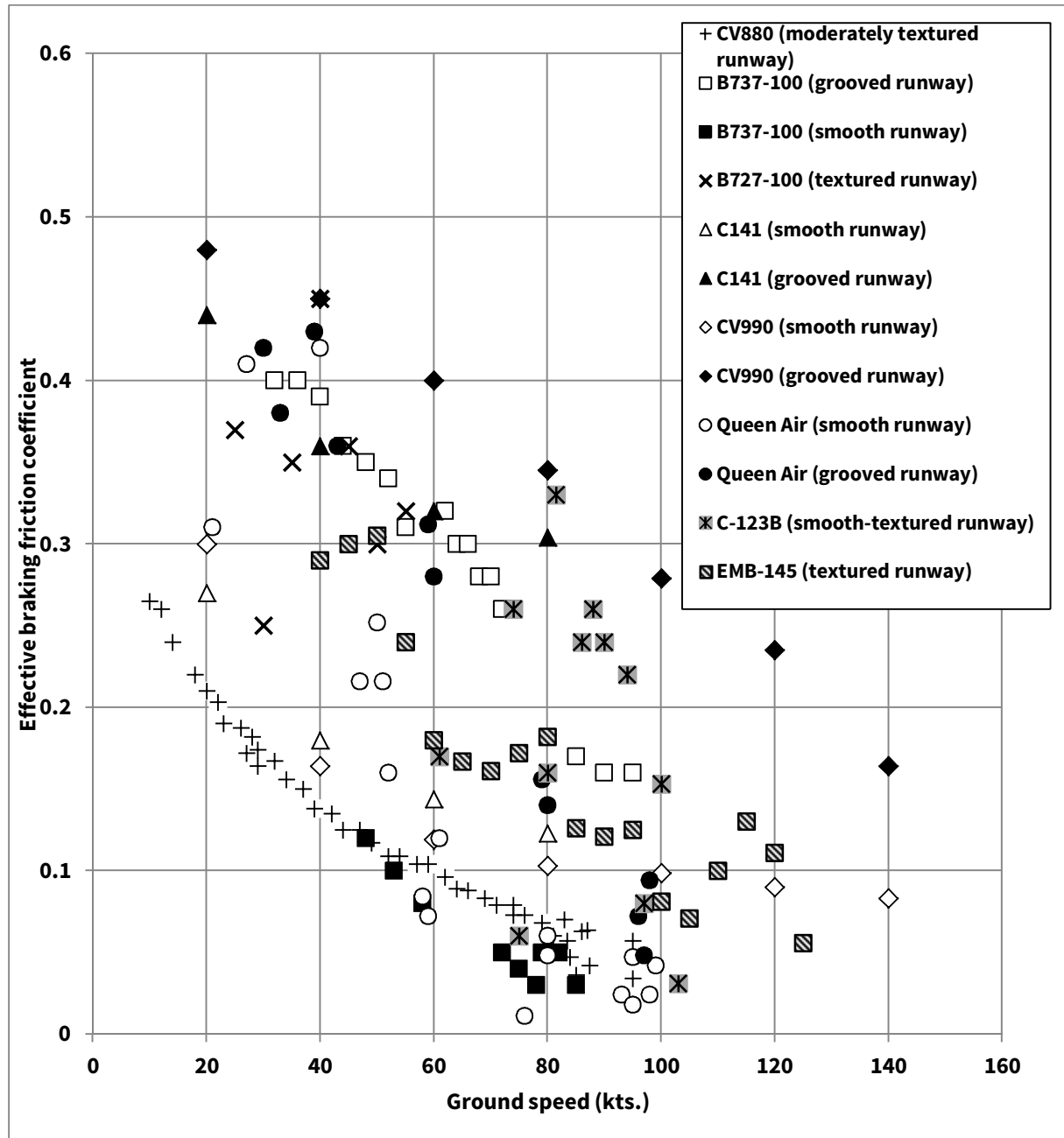


Figure 23: Effective braking friction coefficient as function of ground speed for a range of aircraft on flooded runways.



Figure 24: Example of the Convair CV-880 tested in a specially prepared pond on the runway filled with slush.

The aircraft shown in Figure 23 are all equipped with an anti-skid system except the Queen Air which had no anti-skid device installed. The different anti-skid systems installed have varying levels of efficiency. As a result the effective braking friction coefficient achieved on flooded runways can be very different under the same conditions. This is evident from the data shown in Figure 23. The C-123B had a simple On-Off anti-skid system installed which in this case does show some data points with a remarkable high braking friction value at high speeds. However the variation is very large. The CV-880 was equipped with a Hydro-Aire Mark I anti-skid system. This was one of the earliest modulating anti-skid systems. This system is capable of achieving braking efficiencies of no more than 60-70% on a dry runway a much lower values on a slippery runway. The C-141 and CV-990 were equipped with a more efficient quasi-modulating system (Mark II) resulting in somewhat higher braking efficiencies than for the CV-880. The B737-100 tested by NASA was equipped with a fully modulated anti-skid system (Hydro-

Aire Mark III antiskid system) with an anti-skid efficiency of around 90% on dry runways. The B727-100 used in the NASA tests had a Hydro-Aire Mark II antiskid system with a dry runway anti-skid efficiency of 80% or less. Finally the EMB-145 had the most modern anti-skid system installed of all aircraft in the sample. This system is part of the aircraft's brake-by-wire system and has an efficiency well above 90% for all runway conditions. The friction data for the Embraer EMB-145 are obtained from an accident investigation using the flight data recorders. Such a data acquisition system does not have the same accuracy and high sample rates as the systems installed on test aircraft. Also the accelerometers on normal production aircraft are not always mounted near the centre of gravity which can also introduce errors in the derived braking friction coefficients. Furthermore, the accident investigation revealed signs of reverted rubber hydroplaning on all 4 main tyres of the EMB-145. This can have an influence on the derived friction values. However, the reverted rubber was not present throughout the landing roll. The friction data for the EMB-145 should be used with some caution.

In a number of tests the runway was grooved. Grooves are small channels cut into the surface of existing runways. Grooved runways provide forced water escape from the runway surface under aircraft tyres traveling at high speed [e.g. Daiutole (1979)]. Therefore a higher degree of contact is maintained between the tyres and the runway surface under the condition of a flooded runway. This effect could influence the results shown in Figure 23. A higher braking friction can be experienced at high speeds on a grooved runway than on a non-grooved runway surface with an equivalent macrotexture depth. The effect strongly depends on the shape, size and pitch of the grooves.

5.2.2. Single tyre tests

Figure 25 shows the effective braking friction coefficient of a single tyre on a flooded runway. The test data were obtained from the NASA - Aircraft Landing Dynamics Facility (see Figure 26). All the results are for the same tyre (although obtained through separate tests). This was a VII bias ply tyre with a size of 40 x 14, inflated to 140 psi. The water depth was around 10 mm and the macrotexture around 0.16 mm (smooth surface) in all tests conducted with this tyre type. The results obtained with new tyres (full tread) show a consistent correlation with the ground speed. The small differences are caused by the different type of anti-skid systems used in the different tests. The results obtained with worn tyres are slightly lower than for the new tyres or similar. The effect of the very smooth surface has most likely a bigger influence than the tyre tread. The tread depth in this case was 7.1 mm so the sum of the macrotexture depth and the tread depth was less than the water depth. This explains why there is little difference between the worn and new tyre results.

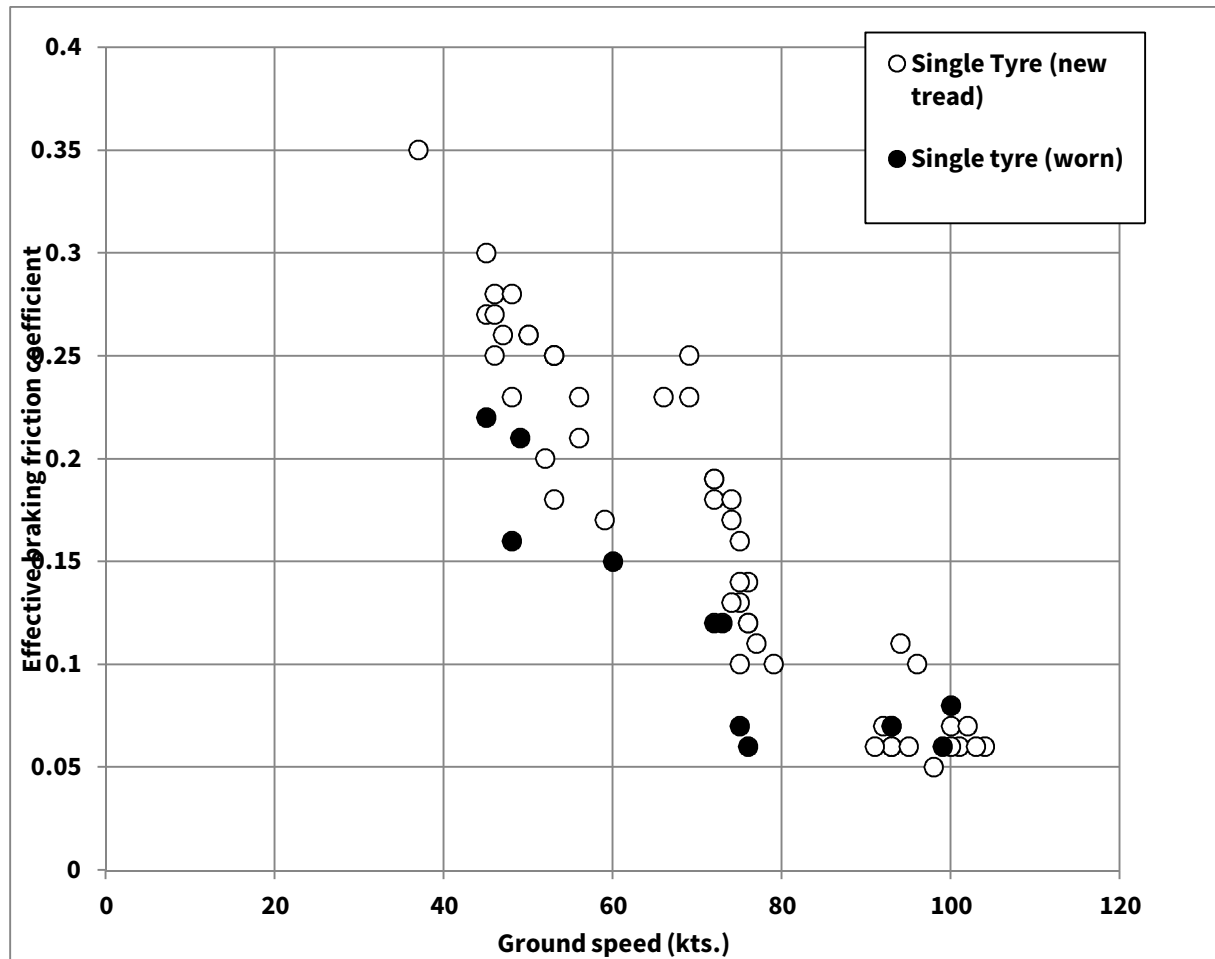


Figure 25: Effective braking friction coefficient of a single tyre on a flooded runway (smooth surfaces).



Figure 26: Picture of the NASA Aircraft Landing Dynamics Facility with the sled with test tyre being launched (source: NASA).

Figure 27 shows a comparison of single tyre tests braking friction results with full scale B737-100 tests results on a smooth flooded runway. The single tyre tests were conducted with the same tyre as used on the B737-100 main landing gear during the NASA flight tests. The runway macrotexture was also the same (0.16 mm in both cases). The average water depth during the B737-100 tests was somewhat less than in the single tyre tests. The tyre inflation pressure of the B737-100 main gear tyres was higher (155 psi) than used for the single tyre tests (140 psi). On flooded runways Zone 1 of the tyre-ground contact area can be large compared with Zones 2 and 3 and at high speeds it may become so large that contact between the tyre and the runway is lost. It is found that increasing inflation pressure tends to offset this effect as the dynamic hydroplaning speed increases with tyre pressure. This could explain the lower braking friction values obtained at the higher speeds. However, the difference at the lower speeds

cannot be explained by this. Most likely a smooth microtexture of the test surface used in the B737-100 tests caused this difference.

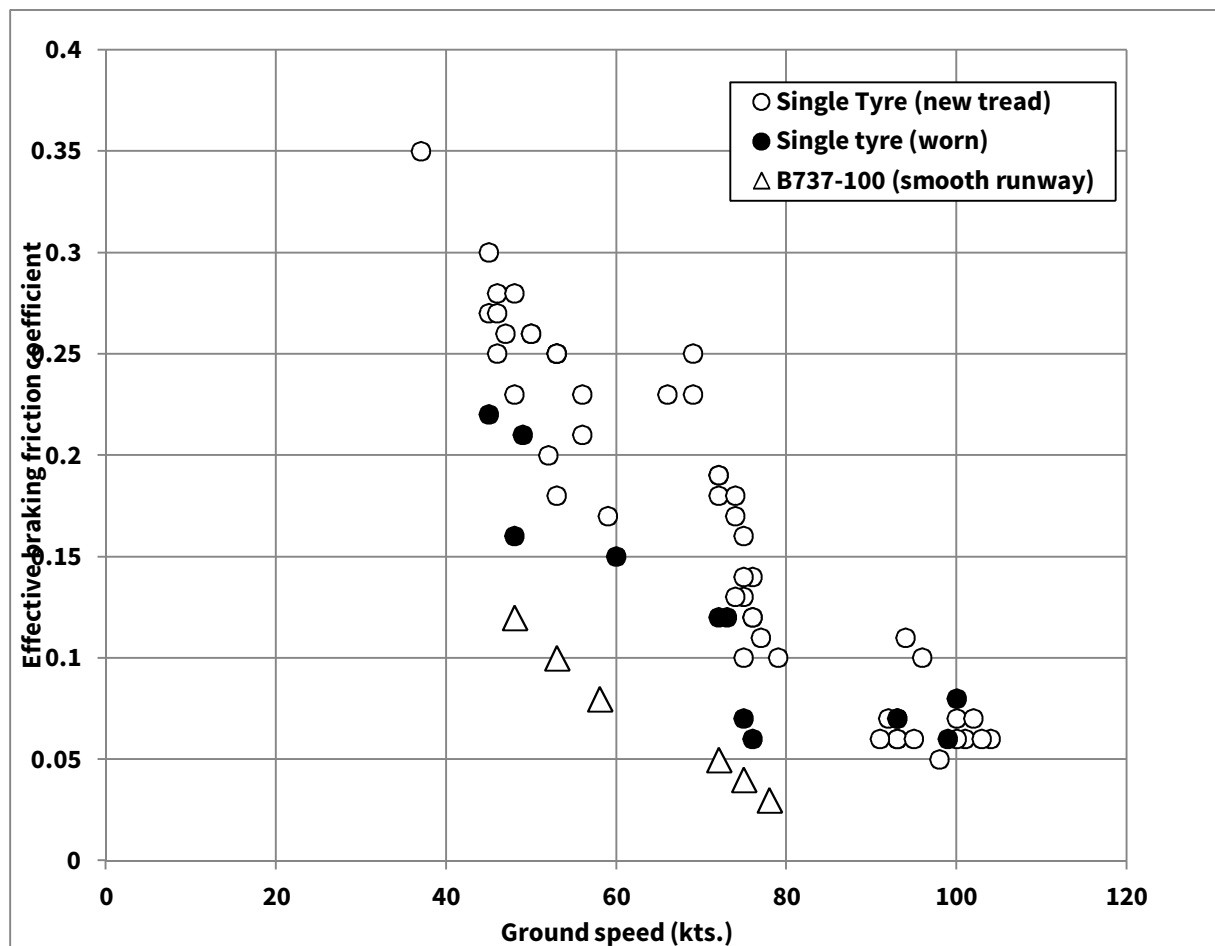


Figure 27: Comparison of single tyre tests braking friction results with full scale B737-100 tests results on a smooth flooded runway.

Figure 28 shows the maximum (peak) braking friction coefficient of different single tyres as function of ground speed on flooded surfaces. These tests were conducted using test facilities without an anti-skid installed. The data shown cover a wide variety of conditions (e.g. tyre tread, inflation pressure, surface texture etc.) making it difficult to compare the data in a single graph. These data can however be used for later analysis assuming typical efficiency values for modern anti-skid systems.

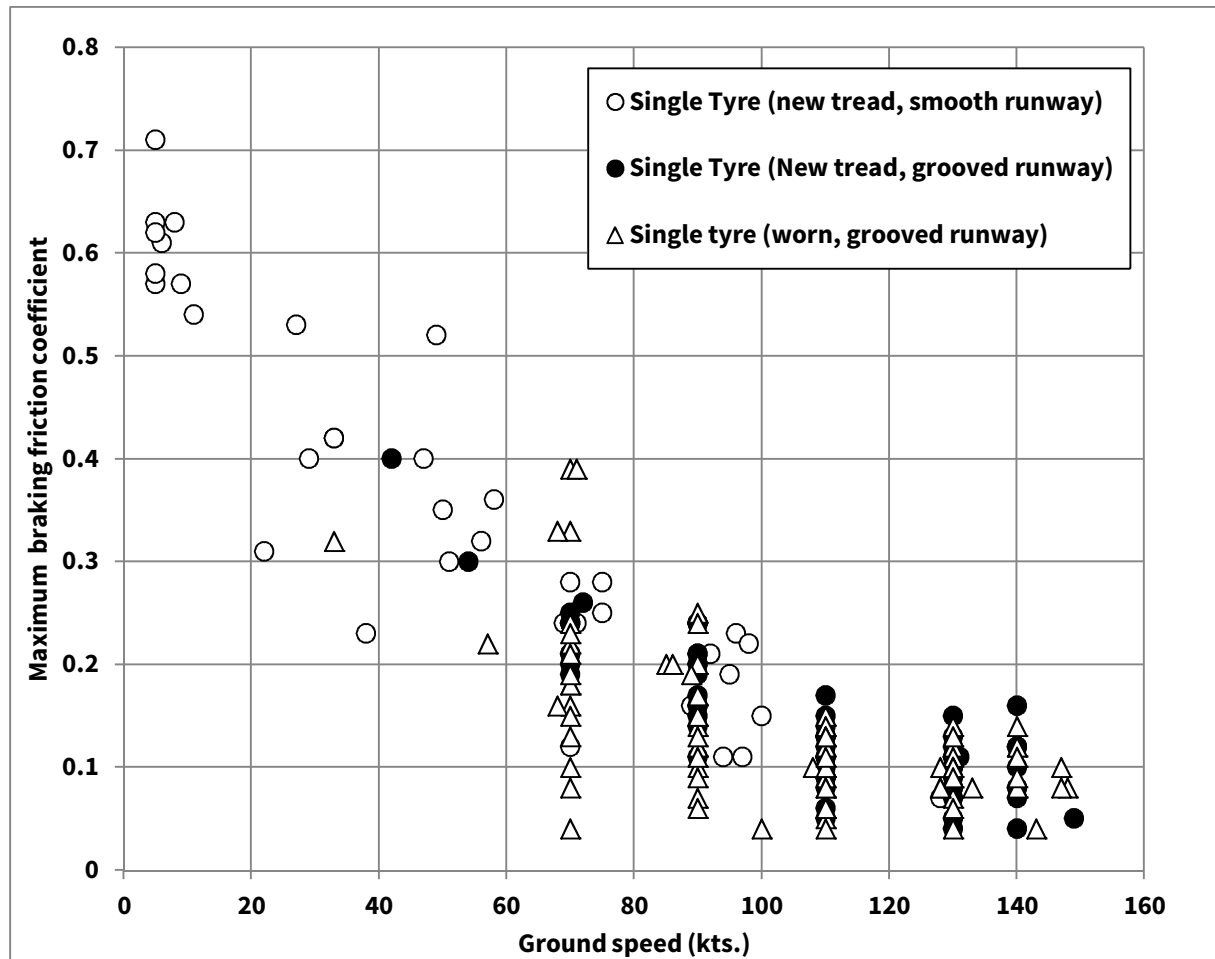


Figure 28: Maximum braking friction coefficient of single tyres on a flooded runway.

5.3. Remarks on the available braking friction data on water contaminated runways

Most of the braking friction data of aircraft tyres on water (or slush) contaminated runways found in the literature for full scale aircraft were obtained with older types of anti-skid systems. These older anti-skid systems have a lower efficiency on flooded runways compared to modern anti-skid systems currently in use. The data obtained with a B737-100 comes close to the performance of current systems. However, this system could still show lower efficiencies on flooded runways compared to dry runways (see e.g. Figure 17). The friction data for the EMB-145 are the only data found for a modern anti-skid system. However, these data were derived from an accident investigation rather than dedicated flight tests.

Data obtained using special tests tracks with single tyres without an anti-skid device could be of interest at a later stage, while correcting the data using typically values for the efficiency of modern anti-skid systems.

No braking friction data were found for radial and H-type aircraft tyres on water contaminated runways.

6 CONCLUSIONS

This report summarises the state of current knowledge regarding tyre braking performance, anti-skid systems, and modern aircraft tyres on water contaminated runways.

The factors that influence aircraft tyre braking performance on water contaminated runways are discussed in detail. Influence of tyre design and runway texture is explained in detail.

Different types of anti-skid systems are presented and their performance on slippery surfaces like water contaminated runways is discussed. This shows that modern anti-skid systems are as efficient on slippery runways (like water contaminated runways) as on dry runways, in contrast to the older anti-skid designs.

Finally experimental data of aircraft tyres braked on water contaminated runways are collected. Both data from full-scale tests as well as data from dynamic load tracks are considered. A database is created with information on recorded braking friction values of a large number of aircraft tyres on water contaminated runways for a range of conditions. This database can be used in later analysis foreseen in task 3.2.3. The now analysed data revealed that there is little information on braking friction on water contaminated runways of aircraft with modern anti-skid systems. The full scale tests with two aircraft foreseen in task 3.2.2 will help to extend the data in this area.

7 REFERENCES

- Allbert, B. J. and Walker, J. C. (1968) Tyre to wet road friction at high speeds. Rubber chemistry and technology, Vol. 41 Nr. 4 Pag. 753-779.
- Agrawal, S.K. (1983) Braking of an Aircraft Tire on Grooved and Porous Asphaltic Concrete, DOT/FAACT-82/147, 1983.
- Agrawal, S.K and Daiutolo, B. (1981) The Braking Performance of an Aircraft Tire on Grooved Portland Cement Concrete Surfaces. Report No. FAA-RD-80-18.
- Alsobrook, C. (1987) Radial Aircraft Tires in Perspective. SAE Technical Paper 871869.
- Attri, N.S. and Amberg, R.L. (1975) Improvements in Airplane Stopping Performance on Adverse Runways. Journal of Aircraft, 1975, Vol.12: 787-790.
- Attri, N. S., Wahi, M. K., Warren, S. M., Amberg, R. L., Straub, H. H., (1974) Combat Traction II, Phase II. Volume II, Detailed Results of Sensitivity Study and Prediction Model Calculations. The Boeing Commercial Airplane Company, ASD-TR-74-41.
- Attri, N.S. (1969) Use of runway condition method to predict braking performance. The Boeing Commercial Airplane Company, Report D6-58384-18TN.
- Baker, D. (2011) Braking Performance Analysis, TSB Canada, Engineering Lab. Report, LP167/2011.
- Bathelt, H.(1973) Die Berechnung des Aquaplaning-Verhaltens von glatten und profilierten Reifen, ATZ, No. 75, 10, pp. 368-374.
- Bathelt, H. (1971) Analytische Behandlung der Strömung in der Aufstandsfläche schnell rollender Reifen auf nasser Fahrbahn ("Aquaplaning"), Dissertation Technische Hochschule Wien.
- Cepic, A. (2004) Hydroplaning of H-Type Aircraft Tyres, SAE Technical Paper 2004-01-3119.
- Charman, M.J. and Rekersdrees, H. (1974) Method of calculation of landing performance for conventional aircraft. Fokker, Report H-O-27.
- Danhof, R.H. (1981) Hydroplaning and coefficient of friction in wet runway testing. Society of Flight Test Engineers, Journal, vol. 3, p. 28-40.
- Daiutole, H. and Grisel, C. (1981) Braking Performance of a United States Air Force Four-Groove 49 X 17 Aircraft Tire With and Without Sipes. Report No. FAA-RO-80-136.
- Daiutole, H. (1979) Braking performance of a Boeing 727 aircraft tire on grooved Portland cement concrete surfaces NAFEC TECHNICAL LETTER REPORT, A-79-19-LR.
- DeVlieg, G.H. et. al. (1992) Landing on Slippery Runways. Boeing Airliner Magazine, Edition October/December.

- Dreher, R.C and Horne, W.B. (1963) Phenomena of Pneumatic Tyre Hydroplaning, NASA TN D-2056.
- Dreher, R. C.; Tanner, J. A. (1974) Experimental investigation of the braking and cornering characteristics of 30 x 11.5-14.5, type 8, aircraft tires with different tread patterns, NASA-TN-D-7743.
- Elliot, R.L. and DeVlieg, G.H. (1978) Landing on slippery runways. The Boeing Commercial Airplane Company, Technical report, D6-44247.
- ESDU (1972) Frictional and retarding forces on aircraft tyres. Part III: planing. Engineering Science data Unit, ESDU 72008.
- Hanson, D.I. (2009) Techniques for Prevention and Remediation of Non-Load Related Distresses on HMA Airport Pavements (Phase I), Airfield Asphalt Pavement Technology Program, Project 05-07.
- Holmes, K.E. (1970) Braking force/braking slip: measurements over a range of conditions between 0 and 100 per cent slip. Road research Lab., Report LR292.
- Horne, W.B. and Buhlmann, F. (1983) A Method for Rating the Skid Resistance and Micro/Macro-texture Characteristics of Wet Pavements, ASTM International STP No. 793, American Society for testing and materials.
- Horne, W.B. and Leland, T.J.W. (1962) Influence of tire tread pattern and runway surface condition on braking friction and rolling resistance of a modern aircraft tire. NASA TN-D-1376.
- Horne, W.B. (1972) Wet runways. NASA TM X-72650.
- Horne, W. B. and Upshur, T.J. (1965) Pneumatic Tyre Hydroplaning and Some Effects on Vehicle Performance., SAE paper 650145.
- Horne, W. B.; Phillips, W. P.; Sparks, H. C.; Yager, T. J. (1970) A Comparison of Aircraft and Ground Vehicle Stopping Performance on Dry, Wet, Flooded, Slush-, Snow-, and Ice-Covered Runways, NASA-TN-D-6098.
- Horne, W.B. et. al. (1965) Recent research on ways to improve tyre traction on water, slush or ice. AIAA Paper No. 65-749.
- l'Anson, R.(1973) An Investigation of Dynamic Aquaplaning Using Small Pneumatic tyres. Ph. D. thesis, University of Bristol.
- Joyner, U.T. and Horne, W.B. (1971) Determining Causation of Aircraft Skidding Accidents or Incidents, Annual Corp. Aircraft Safety Seminar, Washington D.C.
- Lester, W. G. S. and Phil, D. (1973) Some Factors Influencing the Performance of Aircraft Anti-Skid Systems. Tech. Memo. EP 550, R.A.E Royal Aircraft Establishment.
- Logan, J. (2012). Modélisation des forces de contact entre le pneu d'un avion et la piste. DOCTORAT DE L'UNIVERSITÉ DE TOULOUSE.

- Mitchell, D. (1995) Frictional and retarding forces on aircraft tyres. Part II: estimation of braking force. Amendment (D), issued 1, ESDU data Item 71026.
- Moore, D.F. (1966) Prediction of Skid-Resistant Gradient and Drainage Characteristics of Pavements, Highway Research Record 131, Highway Research Board, Washington, D.C., pp. 181-203.
- Niskanen, A and Tuononen, A. (2014). Three 3-axis accelerometers fixed inside the tyre for studying contact patch deformations in wet conditions, Vehicle System Dynamics: International Journal of Vehicle Mechanics and Mobility.
- Nybakken, G.H., Staples R.J and Clark, S.k. (1969) Laboratory Experiments of Reverted Rubber Friction, NASA Contractor Report CR-1398.
- SAE, (2012) Information on Antiskid Systems, Aerospace Information Report, AIR1739B.
- Sawyer, R. H. and Kolnick, J.J. (1959): Tire-to-Surface Friction-Coefficient Measurements with a C-123B Airplane on Various Runway Surfaces. NASA-TR-R-20.
- Schmit, G. (1985) Hydroplaning of aircraft tyres, Goodyear Aircraft Tyres.
- Shrager, J. J. (1962) Vehicular Measurements of Effective Runway Friction. Final Report, Project No. 308-3X (Amendment No. I), FAA.
- Sommers, D. E. et. al. (1962) Runway slush effects on the takeoff of a jet transport; final report. FAA, National Aviation Facilities Experimental Center Atlantic City N J, Project No. 308-3X.
- Straub, H. H. ; Yurczy K.R. F. ; Attri, N. S. (1974) Development of a Pneumatic-Fluidic Antiskid System. The Boeing Commercial Airplane Company, Report.
- Stubbs, S. M. and Tanner, J. A. (1977) Behavior of aircraft antiskid braking systems on dry and wet runway surfaces : a slip-ratio-controlled system with ground speed reference from unbraked nose wheel, NASA technical note ; D-8455.
- Stubbs, S. M. and Tanner, J. A. (1976) Behavior of aircraft antiskid braking systems on dry and wet runway surfaces - A velocity-rate-controlled, pressure-bias-modulated system, NASA TN D- 8332.
- Stubbs, S. M.; Tanner, J. A.; Smith, E. G. (1979) Behavior of aircraft antiskid braking systems on dry and wet runway surfaces. A slip-velocity-controlled, pressure-bias-modulated system, NASA TP-1051.
- Tanner, J. A.; Stubbs, S. M.; Smith, E. G (1981) Behavior of aircraft antiskid braking systems on dry and wet runway surfaces: Hydromechanically controlled system, NASA-TP-1877.
- Tanner, J.A. (1972) Performance of an aircraft tire under cyclic braking and of a currently operational antiskid braking system, NASA TN-D-6755.
- Tanner, J.A. (1982) Review of NASA Antiskid braking research. SAE paper 821393.

- Torenbeek, E. (1982) Synthesis of Subsonic Airplane Design, Delft University Press.
- Van Es, G.W.H. (2001) Hydroplaning of modern aircraft tyres. National Aerospace Laboratory NLR. NLR-TP-2001-242.
- Van Es, G.W.H. and Giesberts, M. (2003) A Literature Survey on Tyre Surface Friction on Wet Pavements Application of Surface Friction Testers. CROW report 03-06, (also published as National Aerospace Laboratory NLR report CR-2002-604).
- Yager, T.J et. al. (1990) Evaluation of two transport aircraft and several ground test vehicle friction measurements obtained for various runway surface types and conditions. A summary of test results from joint FAA/NASA Runway Friction Program. NASA-TP-2917.
- Yager, T.J. et. al. (1968) Effects of pavement texture on wet—runway braking performance. NASA TN D-4323.
- Yager, T. J.; Phillips, W. P.; Deal, P. L. (1971) Evaluation of breaking performance of a light, twin-engine airplane on grooved and ungrooved pavements, NASA-TN-D-6444.
- Yager, T.J. et. al. (1992) Braking, Steering, and Wear Performance of Radial-Belted and Bias-Ply Aircraft Tires, SAE Technical Paper 921036.
- Yager, T. J. and Dreher, R. C. (1976) Traction Characteristics of a 30 by 11.5-14.5, Type 8, Aircraft Tire on Dry, Wet and Flooded Surfaces. NASA-TM-X-72805.
- Yager, T. J. and McCarty, J. L., (1977) Friction characteristics of three 30 by 11.5-14.5, type 8, aircraft tires with various tread groove patterns and rubber compounds, NASA TP-1080.
- Yager, T.J. et. al. (1990) Aircraft Radial-Belted Tire Evaluation, SAE Technical Paper 901913.